March 2018

MECHANISM OF REGULATION OF KINESINS EG5 AND KIF15 BY TPX2

Sai Keshavan Balchand

MECHANISM OF REGULATION ON KINESINS EG5 AND KIF15 BY TPX2

A Dissertation Presented

by

SAI KESHAVAN BALCHAND

Submitted to the Graduate School of the
University of Massachusetts Amherst in partial fulfillment
of the requirements for the degree of

DOCTOR OF PHILOSOPHY

February 2018

Molecular and Cellular Biology

MECHANISM OF REGULATION OF KINESINS EG5 AND KIF15 BY TPX2

A Dissertation Presented

by

Sai Keshavan Balchand

Approved as to style and content by:

Patricia Wadsworth, Chair

Wei – Lih Lee, Member

Thomas J. Maresca, Member

Jennifer L. Ross, Member

Department Director
Molecular and Cellular Biology

DEDICATION

To my Parents, Brother, Swetha, Teachers, Family, Friends and Baba

ACKNOWLEDGEMENTS

I sincerely thank my advisor Patricia Wadsworth for providing me constant guidance throughout my graduate study and providing me invaluable support during difficult times. I also express my deepest gratitude to my committee members Wei-Lih Lee, Tom Maresca and Jenny Ross for insightful inputs and discussions whenever I encountered challenges on my projects. Without my advisor and my committee members' support, I would not be where I am today and for that I am forever grateful.

I sincerely thank members of Wadsworth, Lee, Maresca and Ross lab (past and present) for helpful discussions be it research or abstract, helping with reagents, training me to use new equipment in their labs. I specifically thank Barbara for collaborating on many of the experiments, never giving up on some difficult experiments and for introducing me to the game of thrones. I thank Anna for the all interesting discussions about research, tips for getting better in badminton and the wonderful cupcakes. I thank Abla, Genevieve, Heidi, Aditya and all my roommates for the many happy memories in Amherst.

I cannot thank my parents and brother enough for all their encouragement and moral support throughout my study. I thank my friends Sundar and Manoj who I have known from my undergrad days for making life fun filled during my graduate study. I thank all my relatives for their continuous encouragement. Special thanks to DV and his family for being there and making me feel completely at home over the past few years. I also want to thank all my friends I have made here at UMass for all the memorable moments which I will cherish forever. I finally thank Baba for being there always and guiding from within.

ABSTRACT

MECHANISM OF REGULATION OF KINESINS EG5 AND KIF15 BY TPX2

FEBRUARY 2018

SAI KESHAVAN BALCHAND, B.TECH., ANNA UNIVERSITY CHENNAI

Ph.D., UNIVERSITY OF MASSACHUSETTS AMHERST

Directed by: Professor Patricia Wadsworth

Cell division is the fundamental process by which the replicated genetic material is faithfully segregated to form two identical daughter cells. The mitotic spindle is the macromolecular cytoskeletal structure that is built during every round of cell division to successfully separate the duplicated genome equally into the daughter cells. Errors in spindle formation can thus cause genetic aberrations and can potentially lead to cancer. Understanding the mechanisms that govern proper spindle assembly and function is thus important. Eg5 and Kif15 are two important kinesins which play a major role in establishing and maintaining bipolarity of the mitotic spindle. Both Eg5 and Kif15 have been shown to be regulated by the spindle assembly factor Targeting Protein for Xklp2, or TPX2 the mechanistic details of which remains less clear. The studies presented in this dissertation are aimed at understanding how TPX2 regulates Eg5 and Kif15 using a combination of *in vitro* reconstitution experiments and live cell imaging.

The microtubule co-sedimentation experiments show that removal of the Eg5 interaction domain located on the C-terminus of TPX2 does not abolish the microtubule binding ability of TPX2. My data show that the microtubule binding of TPX2 is

electrostatic but does not involve the negatively charged tubulin E-hook region. In *in vitro* reconstitution Total Internal Reflection Fluorescence (TIRF) experiments, the Eg5-EGFP molecules derived from mammalian cells extracts display biophysical properties similar to the purified Eg5-EGFP molecules. In single molecule TIRF assays, full length TPX2 inhibited Eg5 motion on microtubules and removal of the Eg5 interaction domain from the C-terminus of TPX2 (TPX2-710) significantly reduced the inhibitory effect of TPX2 on Eg5. Data from microtubule surface gliding assays using monomeric and dimeric Eg5 molecules show that dimerization of Eg5 or the residues located in the neck and stalk region of Eg5 are important for the interaction of TPX2 with Eg5. These results suggest that both microtubule binding and ability of TPX2 to interact with Eg5 contribute to the regulation of Eg5 by TPX2.

My data show that the presence of C-terminus of TPX2 enhances Kif15 recruitment of Kif15 onto spindle microtubules and is also required for Eg5 independent bipolar spindle assembly. Characterization of Kif15-GFP molecules from cell extracts suggest that the motor molecules exist as tetramers. In single molecule TIRF experiments, only full length TPX2 suppresses Kif15 motor walking but not the C-terminally truncated TPX2-710. In live cells, fluorescent Kif15-GFP puncta stream towards microtubule plus-ends at rates consistent with microtubule growth rates. Treatment with Paclitaxel suppresses the motility of Kif15 puncta suggesting that dynamic microtubules contribute to the Kif15 behavior in cells. These results offer some mechanistic insights into how TPX2 regulates both the motors Eg5 and Kif15 through its C-terminus.

TABLE OF CONTENTS

LIST OF FIGURES

CHAPTER 1

INTRODUCTION

1.1 Overview of cell division

Biology of all living entities is defined by their ability to utilize energy for growth, interact with and adapt to the surrounding environment and reproduce. So, heritable traits that offer a competitive advantage in performing these functions more efficiently must be passed on faithfully to the next generation without errors. Hence, error free replication of genetic material and its subsequent segregation into its progeny assumes importance.

Multicellular organisms utilize a unique type of cell division called mitosis to create two identical copies of the mother cell. During every round of mitotic cell division, the DNA is replicated and segregated equally to two daughter cells by building a self-assembling structure called the mitotic spindle. The mitotic spindle is a macromolecular structure comprised of a large number of proteins. The skeletal framework of the spindle is formed by microtubules, which are dynamic polymers comprised of tubulin subunits. The microtubules get attached to specific sites on the duplicated chromosomes called kinetochores and separate the sister chromatids and help segregate the two sets of chromosomes to the opposite ends of the cell. Errors during this segregation process can lead to aneuploidy which is frequently observed in cancer. The microtubule cytoskeleton undergoes extensive structural reorganization during different stages in the cell cycle to remain robust and correct errors that may arise before segregation and successfully maintain genetic identity between the newly formed daughter cells.

1.2 Properties of microtubules

Tubulin exists in the soluble fraction of cytosol as an obligate heterodimer comprised of one α and one β tubulin subunit. The heterodimers associate end to end through non covalent interactions forming a protofilament. Lateral interactions between the tubulin monomers in the protofilament results in the formation of a higher order structure namely the microtubule which is comprised of 13 protofilaments wound around a hollow core (Ledbetter and Porter., 1963; Ledbetter and Porter 1964).

The growth of microtubules is governed by the recruitment of tubulin monomers from the solution to the ends of the protofilaments. However, the two ends of microtubules have dissimilar rates of polymerization thus making microtubules polar filaments with a fast growing plus end and a slow growing minus end. The plus end has an exposed β tubulin and the minus end has an exposed α tubulin subunit (Mitchison TJ., 1993). This also gives a defined structural polarity to the microtubules. Tubulin polymerization is also coupled with hydrolysis of the guanosine triphosphate nucleotide associated with the tubulin monomers (Mitchison, 1993). The catalytic hydrolysis of this nucleotide generates structural changes that destabilize the lateral interactions between protofilaments resulting in disassembly of the microtubules (Mitchison and Kirschner, 1984). The rate of nucleotide hydrolysis is slower than the polymerization and hence the microtubules grow faster after nucleation. As the available pool of soluble tubulin decreases due to polymerization, the growth rate slows and the rate of GTP hydrolysis catches up resulting in disassembly. Thus, the constant assembly and disassembly of microtubules during steady state gives the microtubule cytoskeleton an ability to self-

organize and be malleable to reorganization in response to external stimuli (Mitchison and Kirschner, 1984).

During interphase, the microtubules are nucleated and arranged radially around the microtubule organizing center (MTOC) with the minus ends anchored at the MTOC and the plus ends directed towards the periphery of the cells (Borisy et al., 1978; Heidemann et al., 1980; Euteneuer et al., 1981). In mammalian cells, the centrosome functions as the MTOC and is composed of a pair of centrioles surrounded by pericentriolar material. The interphase microtubules are still dynamic, switching between assembly and disassembly (Mitchison and Kirschner, 1984). As the cell enters S phase, the centrosomes are duplicated along with DNA and the duplicated centrosomes remain closely associated till the beginning of prophase when they separate towards opposite sides of the cell which would later become the opposite poles of poles of the spindle. The microtubules emanating from the centrosomes are highly dynamic especially during mitosis (Rusan et al., 2001). The microtubules attach onto specific sites on chromatin called kinetochores which facilitates the movement of duplicated chromosomes towards the center of the cell between the two centrosomes. The establishment of bipolar symmetry helps ensure the generation of tension at the kinetochores and satisfy the spindle assembly checkpoint following which the separated chromatids move towards the opposite poles of the cell during anaphase. The extensive reorganization of the microtubules from a radial array during interphase to a bipolar structure during mitosis is brought about by the concerted efforts of many proteins that include microtubules, microtubule based motor proteins, other non-motor microtubule associated proteins

called MAPs that regulate dynamics of the microtubule cytoskeleton and the microtubule based motors.

1.3 Overview of microtubule motor proteins in mitosis

The microtubule motor proteins are the family of microtubule binding proteins that can translocate on the microtubule tracks powered by the energy derived from hydrolysis of ATP. As microtubules are structurally polar filaments, motor proteins can be plus end directed or minus end directed with some motors capable of bidirectional motion (reviewed in Hirokawa and Noda, 2008). The ability of motor proteins to traverse microtubules directionally and bind to cargo molecules places them in a unique position to help achieve spatial control and non-random distribution of cellular components (Barlan et al., 2013). The major microtubule based motor proteins that play an important role in cell division include proteins from the kinesin superfamily and cytoplasmic dynein. Checkpoint proteins, chromosomes, and microtubules have been shown to be cargo molecules for some of these motor proteins. Hence, these motor proteins play an important role in spindle organization, chromosome alignment, spindle positioning and checkpoint silencing (reviewed in Welburn, 2012; Raaijmakers and Medema, 2014). Several non-motor microtubule associated proteins can also contribute to mitotic spindle formation by regulating the motor proteins that help reorganize the microtubule cytoskeleton.

1.3.1 Kinesins in cell division

Following the initial discovery of the first kinesin protein (Vale et al., 1985), many kinesin like proteins have been subsequently characterized and arranged into 14

families (Lawrence et al., 2004). Based on sequence, structure and function, most kinesins are organized into different domains namely the motor head, neck linker, stalk region and tail. Sequence analysis has shown that the motor head region is highly conserved whereas the regions of the neck linker, stalk and the tail are highly variable giving functional versatility to the kinesin superfamily. The highly conserved kinesin motor head contains the nucleotide binding pocket and harbors the microtubule binding site. The state of nucleotide hydrolysis is sensed by the binding pocket and has been shown to govern the affinity of the motor head to bind to microtubules (Rice et al., 1999; Sindelar et al., 2002). Position of the motor head either at the N or the C terminus of the primary polypeptide sequence determines whether the motor is plus or minus-end directed. The neck linker serves as a short arm lever and helps transmit the force from the ATP binding pocket when the nucleotide is hydrolyzed to the stalk (Rice et al., 1999; Case et al., 2000). The stalk region of most kinesin like proteins contain residues that participate in coiled coil interactions that help the motor molecules oligomerize. Many kinesins have a variable tail region that binds to different accessory proteins which helps in cargo binding (reviewed in Hirokawa et al., 2009). The extended tail region also harbors sites for protein-protein interactions that help in cargo selectivity and can undergo post translational modifications to achieve temporal control over activity of the motor (Rice et al., 1999). Thus, small modulations in the ATP hydrolytic cycle and non-motor domains can give rise to the large variety of kinesins with different biophysical properties like speed, processivity and load bearing capacity that is customized to suit its function.

To identify all kinesins that have important roles during mitosis, a high throughput siRNA screen in *Drosophila* S2 cells was performed (Goshima et al., 2003). Seven kinesins were found to have a major effect on spindle phenotypes. siRNA against Kinesin-5 homologue Klp61F caused monopolar spindles and prevented cell division. siRNA against kinesins Klp67A [Kinesin-8] and Klp10A [Kinesin-13] also caused monopolar spindles which later resolved to bipolar spindles through Klp61F activity. siRNA against CENP meta [Kinesin-7], Klp3A [Kinesin-4] and Nod [Kinesin-10] caused chromosome misalignment and the effects of motors were found to be additive. Depletion of the minus end directed kinesin Ncd [Kinesin-14] caused splayed poles. From this study, it was also found that functions of some kinesins were redundant and could be compensated by the activity of another motor.

A subsequent high throughput siRNA screen targeting human kinesins in Hela cells identified additional kinesins that are involved in cell division (Zhu et al., 2005). Zhu et al identified 5 additional kinesins on top of the 7 which was also identified in the screen performed by Goshima et al. Kif14 [Kinesin-3] and Kif18A [Kinesin-8] were found to be required for proper chromosome alignment and congression. Kif4A and Kif4B [Kinesin-4 family] were found to have functions in anaphase spindle dynamics. MKLP1 and MKLP2 [Kinesin-6 family] were found to be essential for cytokinesis. Several studies have later identified the functions of these kinesins and their respective roles in cell division in more detail. Kinesin-8 or Kif18A is a plus-end directed kinesin that accumulates at the plus-ends of the kinetochore fibers and modulates the dynamics of the kinetochore microtubules (Stumpff et al., 2012). MCAK or Kinesin-13 localizes at the kinetochores and spindle poles and depolymerizes the microtubule ends to regulate

spindle length and microtubule dynamics (Wordeman et al., 2007). CENP-E or kinesin-7 localizes to kinetochores and walks on the microtubules towards the plus ends thereby pushing the chromosomes towards the spindle equator and plays a critical role in chromosome alignment (Wood et al., 1997; Schaar et al., 1997). Though not identified in many siRNA screens for identifying kinesins with roles in cell division, Kif15 [Kinesin-12] is plus-end directed kinesin that binds to microtubules and has been shown to be required to maintain spindle bipolarity in the absence of Eg5 [Kinesin-5] (Tannenbaum et al., 2009; Vanneste et al., 2009). Thus, the vast array of kinesins control different aspects of microtubule dynamics, reorganization and spindle formation.

1.3.2 Cytoplasmic dynein in cell division

Cytoplasmic dynein is a major minus end directed motor protein that forms a large multiprotein complex. By interacting with a variety of adapter complexes, it performs several important functions during cell division that include spindle positioning, spindle pole organization, microtubule transport in the spindle and removal of mitotic checkpoint proteins from the kinetochores which are microtubule attachment sites located at the centromeres of chromosomes (reviewed in Raaijmakers and Medema, 2015). The minus-end directed force production by cytoplasmic dynein counters the kinesin dependent plus-end directed force to help stabilize the bipolar spindle (Ferenz et al., 2009).

1.4 Roles played by non-motor microtubule associated proteins (MAPs) in cell division

Several non-motor microtubule associated proteins (MAPs) can associate with microtubules and modulate spindle architecture. These proteins, sometimes referred to as structural MAPs, can alter the spindle architecture by interacting directly with the microtubule cytoskeleton or by regulating proteins which help organize the spindle. Some examples of MAPs and their functions are discussed here. MAPs like Targeting Protein for Xklp2 (TPX2) and augmin are necessary for nucleating microtubules around chromosomes without which the density of spindle microtubules is reduced (Gruss et al., 2002; Tulu et al., 2006; Goshima et al., 2008). More recently, TPX2 and augmin have also been shown to be required in the nucleation of nascent microtubules from pre-existing microtubules (Petry et al.,2013; Scrofani et al., 2015). MAPs like End Binding protein 1 (EB1) and XMAP 215 can associate with the growing plus ends of microtubules and modulate polymerization rate (Zanic et al., 2013). EB1 is also required for a host of other proteins to localize at the growing plus ends of the microtubules for its function and thus serves as an important master plus-end tip tracker of microtubules (Komarova et al., 2005). MAPs can bind to microtubules and also increase rescue frequency as evidenced in the case of MAP4 (Holmfeldt et al., 2002). Proteins like CLASPs can also bind to microtubules and alter microtubule dynamics at plus ends (Maiato et al., 2003). MAPs like patronin can bind to minus ends of microtubules and act as a capping protein preventing depolymerization at the minus ends (Goodwin et al., 2010). Some MAPs can bundle selective subset of microtubules like PRC1 which preferentially binds and bundles anti-parallel sets of microtubules (Subramanian et al., 2010). MAPs have also been

shown to regulate the motor localization and function. For example, TPX2 has been shown to regulate the recruitment to the kinesin Eg5 to the spindle and alter its motile properties on microtubules (Eckerdt et al., 2008; Ma et al., 2010; Ma et al., 2011). The MAP She1 has been shown to regulate cytoplasmic dynein activity in *Saccharomyces cerevisiae* (Markus et al., 2012).

With a vast array of proteins that can govern the generation, reorganization, maintenance and efficient functioning of the mitotic spindle, the spindle formation remains robust enough to enable quick changes that allow corrections when errors occur. Many functions in the spindle are carried out by several redundant proteins which contribute to this robustness. Because of presence of multiple proteins with redundant functions, it is possible to achieve a functional spindle by multiple mechanisms though the mechanism of action of these different proteins might be different. Hence, proteins essential in one organism may be dispensable in another organism and can be compensated by another protein.

1.5 Kinesin Eg5

BimC was the first kinesin-5 family member identified in a genetic screen in *Aspergillus* and named thus for causing a "blocked in mitosis" phenotype (Enos and Morris 1990). Homologues of BimC have been identified in different organisms and found to be conserved from yeast to humans (Roof et al., 1992; Sawin et al., 1992; Blangy et al., 1995). BimC proteins are characterized by the presence of a head and a conserved region in the tail called BimC box which gets phosphorylated by CDK during mitosis. Phosphorylation of BimC box helps these proteins bind to spindle microtubules

(Blangy et al., 1995). BimC homologues have been later classified as members of kinesin-5 protein family. In most organisms, the kinesin-5 family of proteins has been shown to be necessary for the separation of the spindle pole bodies or centrosomes after duplication and is thus very important in establishing bipolarity of the spindle early in mitosis. In almost all eukaryotes with the exception of *C.elegans,* Kinesin-5 motors are essential to form a bipolar spindle (Roof et al., 1992; Sawin et al., 1992; Blangy et al., 1995; Hoyt et al., 1992).

Electron micrographs of Drosophila kinesin-5 homologue KLP61F showed that these molecules are homotetramers with two heads each on either end of the molecule separated by a long stalk formed by the coiled coil region giving it an appearance of a dumbbell (Kashina et al., 1996). It was postulated that this characteristic arrangement of motor heads could help kinesin-5 molecules to bind to two microtubule filaments simultaneously and slide them apart generating an outward force to help separate the centrosomes (Kashina et al., 1996) and was later elucidated through *in vitro* reconstitution experiments using purified Eg5 molecules (Kapitein et al., 2005).

The localization of kinesin-5 during interphase is cytosolic. Kinesin-5 gets recruited onto the spindle fibers during cell division by phosphorylation of the BimC box by CDK (Blangy et al., 1995). After recruitment to the spindle early in mitosis, kinesin-5 motors help separate the duplicated centrosomes establishing bipolarity. Removal of kinesin-5 from cells by depletions or small molecule inhibitions give rise to monopolar spindles in most organisms and cells fail to complete mitosis (Mayer et al., 1999, Kapoor et al., 2000). However, it has also been shown that kinesin-5 is not required for maintenance of the bipolarity of the spindle as evidenced by the insensitivity of tissue

culture cells to kinesin-5 inhibitors after establishment of metaphase (Tannenbaum et al., 2009; Ferenz et al., 2010). This suggests that though kinesin-5 is essential for establishment of bipolarity in most organisms, it is dispensable for maintenance of bipolarity. In *S. cerevisiae,* the kinesin-5 homologue cin8 has been shown to be also necessary for maintain a bipolar spindle and avoid collapsing (Hoyt et al., 1992).

In *in vitro* experiments, kinesin-5 molecules have been shown to walk on single microtubules at approximately 20nm/s and are slow motors in comparison with conventional kinesin-1 which walks at speeds greater than 350nm/s (Kapitein et al., 2005; Block et al., 1990). It has also been shown that *Xenopus* Eg5 switches from predominantly diffusive motion on a single microtubule to being highly directed when engaged between two anti-parallel microtubules (Kapitein et al., 2005; Kwok et al., 2006) sliding the microtubules at a maximum rate of 40nm/s. Thus, the kinesin-5 molecules can generate a net outward directed force in the spindle when engaged between overlapping anti-parallel microtubules. This outward force is countered by the minus-end directed motor cytoplasmic dynein (Ferenz et al., 2009). In cells, inhibition of dynein or kinesin-5 alone results in a destabilized spindle. But, inhibition of both motors restores spindle bipolarity suggesting that the balance of forces is necessary for efficient spindle function (Ferenz et al., 2009).

Apart from being post translationally regulated by the kinase CDK, kinesin-5 molecules have been shown to be regulated by the MAP TPX2 (Eckerdt et al., 2008; Ma et al., 2010). TPX2 enhances the localization of kinesin-5 onto spindle fibers in cells and has been shown through *in vitro* experiments to be a negative regulator of Eg5 motion on microtubules thereby potentially regulating its outward force generation (Ma et al., 2011).

Removal of the last 37 residues of TPX2 changes the localization of Eg5 on the spindle microtubules and causes defective spindles suggesting that these residues of TPX2 play a role in regulating Eg5 function (Ma et al., 2011). Thus, the kinesin-5 motors are tightly regulated throughout the cell cycle.

1.6 Kinesin-12 or Kif15

Kinesin-12 or Kif15 is a plus end directed kinesin that was initially discovered as in a siRNA screen to identify proteins playing a role of maintaining the bipolarity of the spindle. In the screen, siRNA treated cells were first arrested in metaphase using MG132, then treated with STLC to inhibit Eg5 and ability of cells to maintain bipolarity was scored (Tannenbaum et al., 2009). While not essential for cell viability under normal conditions, Kif15 becomes necessary for viability when Eg5 function is compromised. In the absence of Eg5, exogenous expression of Kif15 was found to be sufficient to assemble functional bipolar spindles (Tannenbaum et al., 2009; Sturgill et al., 2013).

Kif15 contains a conserved kinesin motor head at its N-terminus and has a long C-terminal tail that contains a leucine zipper domain that helps Kif15 oligomerize. Though Kif15 contains a microtubule binding motor domain, the microtubule binding of Kif15 on the mitotic spindle depends on the presence of the microtubule associated protein TPX2 (Vanneste et al., 2009; Tannenbaum et al., 2009). The C terminal leucine zipper region of Kif15 has also been shown to be necessary for its TPX2 dependent localization onto the spindle microtubules (Tannenbaum et al., 2009). Initial models suggested that TPX2 helps the dimeric Kif15 localize to the spindle microtubules and help maintain bipolarity (Tannenbaum et al., 2009; Vanneste et al., 2009). Recently, it

was also shown that recruitment of Kif15 on the mitotic spindle microtubules is enhanced through post translational modifications mediated by aurora A kinase (Van Heesbeen et al., 2016)

Kif15 has been shown to bind to spindle microtubules and play a role in controlling pre-anaphase spindle length (Tannenbaum et al., 2009; Sturgill et al., 2013). Recent studies have also shown that elevated Kif15 expression can stabilize kinetochore microtubules bundles and help form bipolar spindles when Eg5 function is compromised (Sturgill et al., 2013; Gayek and Ohi, 2014). Purified molecules of Kif15 directly binds to microtubules and processively walk towards plus ends in *in vitro* reconstitution experiments. Kif15 binds to microtubule pairs and can bundle microtubules (Drechsler et al., 2014). Contradicting results have been observed for oligomeric state of purified Kif15 molecules with two groups independently showing the molecule to be a dimer and tetramer respectively (Sturgill et al., 2014; Drechsler et al., 2014). Determination of the oligomeric state of the Kif15 molecules in their native state will help in developing models for the mode of action of Kif15 on the mitotic spindle.

1.7 Targeting protein for Xklp2 (TPX2)

TPX2 was initially discovered to be a factor essential for targeting *Xenopus* kinesin like protein 2 (Xklp2) onto the mitotic spindle poles (Wittmann et al., 1998). TPX2 is a microtubule associated protein that plays several important roles in mitosis and is necessary for cell division across different species (Wittmann et al., 2000; Gruss et al., 2001; Gruss et al., 2002; Garrett et al., 2002; Goshima, 2011). The primary sequence of TPX2 contains a nuclear localization signal near its amino-terminus and thus localizes in

the nucleus during interphase (Trieselmann et al., 2003). After the nuclear envelope breaks down, Ran^{GTP} regulates the release of TPX2 from importin α near the vicinity of chromosomes and TPX2 subsequently localizes on spindle microtubules throughout mitosis (Gruss et al., 2001; Gruss et al., 2002; Schatz et al., 2003).

In cells, TPX2 is one of the necessary components for *de novo* microtubule nucleation around chromosomes and thus plays an important role in the chromatin derived microtubule assembly (Gruss et al., 2002, Tulu et al., 2006, Bird and Hyman, 2008). The role of TPX2 in microtubule nucleation has also been captured in many *in vitro* reconstitution studies. As a microtubule binding protein, TPX2 has been demonstrated to nucleate microtubule asters when incubated with pure tubulin (Schatz et al., 2003; Brunet et al., 2004). In *Xenopus* extracts, TPX2 is required for nucleation of branched microtubules from the sides of existing microtubules (Petry et al., 2013). TPX2 has also been shown to be necessary for Ran GTP mediated microtubule nucleation in *Xenopus* extracts by acting as a scaffold and forming a complex with proteins RHAMM and γTURC (Scrofani et al., 2015). Further, TPX2 can also suppress microtubule assembly kinetics at microtubule plus ends and act synergistically with chTOG to promote microtubule nucleation (Roostalu et al., 2015; Reid et al., 2016).

TPX2 has been shown to be necessary for targeting different spindle assembly factors to the spindle microtubules during cell division. The N terminus of TPX2 binds and activates the kinase aurora A and subsequently targets it to the spindle microtubules (Kufer et al., 2002; Bayliss et al., 2003; Tsai et al., 2003; Eyers and Maller, 2004). TPX2 has also been demonstrated to be necessary for effective spindle localization of kinesins Xklp2 and Eg5 (Wittmann et al., 1998; Eckerdt and Maller, 2008; Ma et al., 2011).

1.8 Motivation for the study

Previous works have identified Eg5 and Kif15 to be the chief plus-end directed force generators in the mitotic spindle and help establish and maintain bipolarity during the assembly process. The MAP TPX2 interestingly plays a role in localization of both these motors on the spindle microtubules and is known to regulate them. The C-terminal amino acid residues of TPX2 are required for interacting with Eg5 and regulating it on the spindle. However, the requirements for TPX2 regulation of Kif15 are not completely understood. The experiments presented in these chapters aim at understanding the regulation of Eg5 and Kif15 by TPX2 at the molecular level using single molecule *in vitro* reconstitution experiments. Understanding this could help elucidate how the same MAP TPX2 regulates two similar motors Eg5 and Kif15 using the same domain.

CHAPTER 2

TPX2 INHIBITS EG5 BY INTERACTION WITH BOTH MOTOR AND MICROTUBULE

This chapter is adapted from Balchand et al., 2015. The TPX2 Halo tag proteins were cloned, purified and labeled by Barbara J Mann. The single molecule TIRF experiments, experiments to determine dwell times of TPX2 and data analysis were performed in collaboration with Barbara J Mann.

2.1 Introduction

Accurate chromosome segregation during cell division requires the assembly and function of the mitotic spindle. The spindle is composed of a bipolar array of dynamic microtubules that are required for chromosome alignment and segregation. Mitotic motor proteins play important roles in regulating microtubule organization and dynamics and in generating the forces required for spindle formation and chromosome motion. Despite the characterization of many mitotic motor proteins, how their activity is regulated both spatially and temporally in the spindle remains incompletely understood (Walczak et al., 2008).

TPX2 is a conserved mitotic microtubule-associated protein (MAP) that was originally identified as a protein required for the dynein-dependent targeting of the Xenopus kinesin Xklp2 to mitotic spindle poles (Wittmann et al., 1998). In mammalian cells, TPX2 localizes to the nucleus in interphase and to the spindle in mitosis with enrichment near spindle poles (Gruss et al., 2002; Garrett et al., 2002). Depletion of

TPX2 using siRNA results in short bipolar or multipolar spindles that fail to progress through mitosis (Gruss et al., 2002; Garrett et al., 2002). The N-terminus of TPX2 binds and activates the mitotic kinase Aurora A and is required to localize the kinase to spindle microtubules (Kufer et al., 2002; Bayliss et al., 2003; Eyers et al., 2004). During spindle formation, TPX2 is required for microtubule formation near kinetochores, an activity that requires GTP-bound Ran, which relieves the inhibitory action of importin α/β on TPX2 (Tulu et al., 2006). In addition, it has been demonstrated that the C-terminus of TPX2 binds to the bipolar kinesin Eg5 and targets the motor to spindle microtubules (Ma et al., 2010; Eckerdt et al., 2008). Expression of TPX2 lacking the C-terminal 35 amino acids, which contribute to Eg5 binding, results in defective spindles with greatly reduced Eg5 on spindle microtubules, unfocussed spindle poles, and bent and buckled microtubules (Ma et al., 2011).

Because Eg5 plays a critical and conserved function in establishing spindle bipolarity, it is important to understand how this motor is regulated in the spindle. Previous *in vitro* experiments have shown that purified TPX2 reduces the velocity of Eg5-dependent microtubule gliding and microtubule-microtubule-dependent sliding (Ma et al., 2011). Eg5 accumulation on microtubules is enhanced in the presence of full-length TPX2, but less in the presence of TPX2 lacking the Eg5 binding domain (Ma et al., 2011). These results directly demonstrate that TPX2 inhibits the ability of Eg5 to translocate microtubules, but the mechanism of inhibition is not established.

In this chapter, I used *in vitro* assays and single molecule TIRF microscopy to characterize the interaction of TPX2 with microtubules and to examine the behavior of Eg5 in the presence of TPX2. The results demonstrate that TPX2 blocks Eg5 motility

both by a direct interaction with Eg5 and by binding to microtubules and acting as a roadblock. Using microtubule gliding assays, I further show that dimeric, but not monomeric Eg5 is differentially inhibited by full-length and truncated TPX2. These experiments provide new insight into the microtubule-associated protein TPX2 and its regulation of the mitotic kinesin Eg5.

2.2 Results

2.2.1 TPX2 Binding to Microtubules

To examine the regulation of mammalian Eg5 by TPX2, purified full-length TPX2 and a truncated version lacking the C-terminal 35 amino acids (referred to as TPX2-710) that mediate the interaction with Eg5 (Eckerdt et al., 2008; Ma et al., 2011) (Fig. 2.1*A*) was expressed and purified from sf9 cells. To characterize the microtubule binding of these proteins, microtubule co-sedimentation experiments were performed. Both full-length TPX2 and TPX2-710 co-sedimented with microtubules with apparent dissociation constants of 125 and 240 nM respectively (Fig. 2.1, *B* and *C*). Both full-length and truncated TPX2 could be released from the microtubule lattice by adding increasing concentrations of KCl to the buffer, with negligible binding observed at 250 mM KCl (Fig. 2.2*A*). This demonstrates that, like many other microtubule-associated proteins, TPX2 makes ionic interactions with the microtubule lattice.

Microtubule-associated proteins are thought to make electrostatic interactions specifically with the negatively charged C-terminal E-hooks of tubulin, named for the abundance of glutamic acid residues in the tail region of tubulin (Paschal et al., 1989). To determine whether the E-hooks are either a requirement for or facilitate TPX2 binding to

microtubules, polymerized microtubules were digested with the enzyme subtilisin A to cleave off the E-hooks. Then, binding of fluorescently labeled Halo-tagged TPX2 and TPX2-710 to control and subtilisin-digested microtubules was measured. The results show that binding of full-length or truncated TPX2 to microtubules was not different for untreated when compared with subtilisin-digested microtubules (Fig. 2.2*B*).

To examine the interaction of individual molecules of TPX2 with the microtubule, single molecule TIRF microscopy of fluorescently labeled Halo-tagged TPX2 full-length and TPX2-710 was performed. Individual molecules were stationary on the microtubule lattice, and at the concentration examined, no enrichment at either end of the microtubule was observed. The average dwell time of full-length TPX2-Halo, measured from image sequences acquired at 2-s intervals for 15 min, was 60.1 s (Fig. 2.2*C*). The average dwell time of Halo-tagged TPX2-710 was 46.6 s and was not statistically different from that of the Halo-tagged full-length TPX2.

Together, these results demonstrate that TPX2 binds to the microtubule lattice with high affinity and that the C-terminal 35 amino acids do not contribute significantly to this interaction. Additionally, TPX2 does not require the tubulin E-hook for microtubule binding, suggesting that other tubulin residues are responsible for the interaction.

2.2.2 Functional Eg5 from Mammalian Cell Extracts

Cytoplasmic extracts (Cai et al., 2007) were prepared from a mammalian cell line stably expressing full-length, localization, and affinity purification- tagged Eg5 (hereafter referred to as Eg5-EGFP) expressed from a bacterial artificial chromosome under control

of the native promoter (Gable et al., 2012; Cai et al., 2007). The concentration of Eg5-EGFP in the cell extracts was determined using Western blotting; values of 20–60 nM were obtained, depending on the extract (Fig. 2.3*A*). The concentration of TPX2 in these cytoplasmic extracts was less than ~1 nM, consistent with the localization of TPX2 to the nucleus during interphase (data not shown).

To analyze Eg5-EGFP motors in cell extracts, the extract was diluted into motility buffer to achieve a final motor concentration of ~1 nM. Diluted extract was added to flow chambers containing rhodamine-labeled, Taxol-stabilized microtubules immobilized to the surface using anti-tubulin antibodies. Using TIRF microscopy, bright puncta were observed to bind to the microtubules in the absence of ATP. Upon the addition of ATP, robust motility of nearly all puncta was observed (Fig. 2.3*B*). Accumulation of motors at one end of microtubules in the field of view was frequently observed (Fig.2.3*B*), indicating that motors remain associated with the microtubule plus-end after motion. This is consistent with the previously observed tethering of microtubules near the microtubule end in sliding assays using *Xenopus* Eg5 (see below) (Kapitein et al., 2005). At higher motor concentrations, microtubules were uniformly coated with fluorescence, and individual puncta could not be resolved. The average velocity of individual puncta was 14.7 ± 0.9 nm/s, (S.E.) (n = 205) similar to the velocity of purified *Xenopus* and *Drosophila* Eg5 motors (Kwok et al., 2006; Kapitein et al., 2008; van den Wildenberg et al., 2008) (Fig. 2.3*D*). The average association time of Eg5 with the microtubules was not determined because motors rarely dissociated over the course of a 10-min movie, and longer movies resulted in photobleaching of individual puncta. Finally, motor behavior was not altered following storage in liquid nitrogen for several weeks, so a single extract

could be used for multiple experiments, making this a robust and versatile method for studying motor behavior.

To determine the directionality of motor motion, kinesin-1-EGFP, a plus-end-directed motor, was added to the chamber, and the direction of motion was observed. Next, the chamber was washed with 5 chamber volumes of ATP-containing motility buffer to remove the kinesin-1-EGFP. Eg5-EGFP was added to the same chamber, and motor behavior was followed in the same field of view. In all cases, both kinesin-1-EGFP and Eg5-EGFP moved to the same end of the microtubule (Fig. 2.3*C*), demonstrating that the motile Eg5 puncta in the mammalian cell extract walk to the microtubule plus-end.

Next, a single molecule TIRF microscopy based method was used to determine whether the Eg5-EGFP motors in the extract were present as tetramers. Because the cells expressing Eg5-EGFP also express endogenous Eg5, the motile motors could be composed of between one and four EGFP molecules. In this cell line, the Eg5-EGFP is not resistant to the siRNA designed to deplete endogenous Eg5 (Gable et al., 2012). Therefore, to estimate the number of labeled Eg5 motors in the motile puncta, endogenous Eg5 was depleted from parental cells cotransfected with siRNA-resistant Eg5-mEmerald and prepared cell extracts two days after transfection. The average fluorescence intensity of individual Eg5-mEmerald puncta was measured and compared with the fluorescence intensity of bacterially expressed kinesin-1-EGFP dimers imaged under identical conditions on the same day (Fig. 2.3*E*). On average, the Eg5-mEmerald puncta was twice as bright as the kinesin-1-EGFP dimers, indicating that Eg5 was predominately tetrameric. The increase in quantum fluorescence yield of mEmerald alone is not sufficient to explain the nearly 2-fold increase in fluorescence intensity (Day et al.,

2009). Additionally, the siRNA may not deplete 100% of the endogenous Eg5, which could form tetramers with the Eg5-mEmerald, resulting in decreased observed fluorescence for some puncta.

To determine whether the Eg5-EGFP molecules function as tetramers, the ability of Eg5-EGFP from extracts to cross-link and slide two microtubules was examined. To do this, Eg5-EGFP was added to immobilized microtubules in a flow chamber and then added additional microtubules. The added microtubules bound to the immobilized microtubules and were translocated upon the addition of ATP, demonstrating that Eg5-EGFP was capable of cross-linking and sliding microtubules (Fig. 2.3*F*). In addition, the moving microtubule remained associated with the tip of the immobilized microtubule, consistent with previous observations (Kapitein et al., 2005). Together, these experiments demonstrate that Eg5-EGFP from extracts is tetrameric (Fig. 2.3, *E* and *F*).

Next, size exclusion chromatography was performed on the extracts from LLC-Pk1 cells. Due to the low abundance of Eg5-EGFP in these extracts, cells overexpressing Eg5-mEmerald were used to aid in the detection. The Western blots of the fractions obtained show that Eg5-mEmerald elutes around the same fractions as the Eg5-EGFP molecules, which are purified from SF9 insect cells, suggesting that the Eg5 molecules obtained from cell extracts are tetramers (Fig. 2.3*G*). To demonstrate that the bright motile puncta derived from the cell extract are Eg5 molecules, *S*-trityl-L-cysteine (STLC) or 2-[1-(4-fluorophenyl)cyclopropyl]-4-(pyridin-4-yl)thiazole (FCPT) was added in single molecule experiments, which specifically inhibit Eg5 (Groen et al., 2008; Skoufias et al., 2006). Each inhibitor completely stopped the motion of motile puncta (Fig.2.3*H*); in the presence of FCPT, motors remained bound to the microtubule lattice, whereas in

the presence of STLC, motors stopped walking and in many cases were released from the microtubule (Kwok et al., 2006) (Fig. 2.3*H*).

Eg5 has been shown to exhibit diffusive behavior on microtubules at physiological salt concentration (Kwok et al., 2006; Weinger et al., 2011). To determine whether mammalian Eg5 present in diluted cell extracts showed similar diffusive behavior, increasing concentrations of KCl was added to the motility buffer and motor behavior was examined. At 20 mM KCl, the velocity of Eg5 was 12.1 nm/s, similar to that observed in 0 mM KCl, and the diffusion coefficient, *D*, obtained from plots of MSD over time, was 1588nm2/s. At 50 mM KCl, motor velocity dropped to 3 nm/s, and the value of *D* was 4556 nm2/s (Fig. 2.3*I*). These results demonstrate that motor processivity is dependent on the ionic conditions, consistent with previous results using *Xenopus* Eg5 (Kapitein et al., 2008; Weinger et al., 2011).

Together, these results show that Eg5-EGFP motors in mammalian cell extracts behave in a manner similar to purified *Xenopus* and *Drosophila* Eg5 tetramers. Specifically, the velocity, directionality, sensitivity to STLC and FCPT and diffusive behavior in higher ionic strength buffer are all consistent with previously reported properties of purified *Xenopus* and *Drosophila* kinesin-5 motors. The data presented here suggest that these motors are similar to insect and other vertebrate Eg5 motors and distinct from kinesin-5 motors from yeast that show directional switching (Roostalu et al., 2011; Gerson-Gurwitz et al., 2011). Importantly, the similar properties of the mammalian motors strongly suggest that other components that are present in the cell extract do not have a major effect on motor behavior.

2.2.3 Interactions of TPX2 with the Microtubule and with Eg5 Both Contribute to Inhibition of Motility

Previous work demonstrated that the gliding of microtubules by surface-attached Eg5 dimers is inhibited by full-length TPX2 and to a lesser extent by TPX2-710 (Ma et al., 2011). Full-length TPX2 also inhibits Eg5-mediated microtubule-microtubule sliding (Ma et al., 2011). In both of these assays, however, the behavior of populations of motors was examined, so how individual Eg5 molecules are regulated by TPX2 was not revealed. To gain a better understanding of the mechanism of inhibition of Eg5 by TPX2, single molecule TIRF experiments were performed combining Eg5 and TPX2 in the assay.

To determine the effect of TPX2 on Eg5 behavior, the cytoplasmic extract containing Eg5-EGFP was diluted in motility buffer and added to chambers of immobilized microtubules, and motors were imaged. Next, TPX2 was added to the chamber during image acquisition (Fig. 2.4*A*). For these experiments, the velocity of motors following the addition of TPX2 is expressed as a percentage of the velocity prior to the addition of TPX2. The data show that full-length TPX2 is a potent inhibitor of the velocity of individual Eg5 motors; at 250 nM, TPX2 reduced Eg5 velocity by 83%, and at 50 nM, Eg5 velocity was reduced by 32% (Fig. 2.4*B*).

To understand how the interaction of TPX2 with Eg5 contributes to motor inhibition, the experiment was repeated using TPX2-710. The addition of TPX2-710 also substantially reduced the velocity of Eg5-EGFP, indicating that microtubule binding by TPX2 contributes to the reduction in motor velocity. At low concentrations (50 nM), both

TPX2 and TPX2–710 showed similar inhibition of Eg5 (32 and 24%, respectively). However, at higher concentrations (250 nM), TPX2-710 was a less effective inhibitor of Eg5-EGFP than full-length TPX2 (inhibition of 53 and 83%, respectively) (Fig. 2.4*B*).

The results further show that TPX2 reduces the velocity of Eg5-EGFP motors without inducing dissociation of most motors from the microtubule (Fig. 2.4*A*), consistent with the established role of TPX2 in targeting Eg5 to spindle microtubules (Ma et al., 2011). In the presence of TPX2-710, more motors appeared to dissociate from the microtubule, although photobleaching precluded accurate quantification. In some cases, following the addition of TPX2 to the motility chamber, motors from solution associated with the microtubule, and these motors also moved with reduced velocity (Fig. 2.4*A*).

To confirm the specificity of the Eg5-TPX2 interaction, full-length TPX2-Halo covalently tagged with an Alexa 660 ligand was added to kinesin-1-EGFP dimers in a single molecule assay (Fig. 2.4*C*). Consistent with prior results from microtubule gliding assays, TPX2 addition did not alter the motility of kinesin-1-EGFP (Ma et al., 2011).

To visualize the interaction between Eg5 and TPX2 in the single molecule experiments, TPX2-Halo covalently tagged with an Alexa 660 ligand was used (Fig. 2.4*D*). In this experiment, the addition of TPX2-Halo (at 20 nM) reduced the velocity of Eg5-EGFP. Analysis of kymographs showed that individual motors that encountered TPX2-Halo walked at reduced velocity. In some cases, a motor that shows reduced velocity can resume motion when it encounters an area of the microtubule that is relatively free of TPX2 (Fig. 2.4*D* (*right panels*)).

Experiments were also performed by premixing the motor and MAP where 50 nM TPX2 or TPX2-710 was premixed with the motor in motility buffer before addition to the chamber. This method allows Eg5 and TPX2 to potentially interact in solution, and both molecules are introduced to the chamber simultaneously (Fig. 2.4, *E* and *F*). This experiment also showed greater inhibition of Eg5-EGFP by the full-length compared with the truncated TPX2 (Fig. 2.4, *E* and *F*). Interestingly, premixing full-length TPX2 with Eg5-EGFP resulted in greater inhibition than when the same concentration of TPX2 was added to motors pre bound to microtubules (60% *versus* 32% inhibition; Fig. 2.4, *B* and *F*). This result indicates that when the motor and TPX2 bind to the microtubule at the same time, stronger inhibition results. In contrast, when TPX2 is added to motors already bound to microtubules, TPX2 can bind to the microtubule at sites distant from the motors and thus not immediately impact motor velocity. Interestingly, in the case of TPX2-710, inhibition of Eg5-EGFP was similar regardless of whether the motors were premixed or added sequentially (Fig. 2.4, *B* and *F*).

Finally, to exclude the possibility that adding a Halo tag to TPX2 affected the TPX2-Eg5 interaction, as a control, inhibition of Eg5 by untagged and Halo-tagged TPX2 was compared through single molecule experiments. As seen in Fig.2.4*F*, inhibition of Eg5-EGFP by TPX2 was not changed by the presence of the Halo tag, demonstrating that the Halo tag was not detectably affecting TPX2-Eg5 interaction (Fig. 2.4*F*).

Together, the results of these experiments demonstrate that Eg5 in cytoplasmic extracts is inhibited by TPX2. Full-length TPX2, which can interact with Eg5 and with the microtubule, is a more potent inhibitor than TPX2-710, which lacks the Eg5

interaction domain. However, by binding to the microtubule lattice, TPX2-710 also substantially reduces the velocity of individual Eg5 puncta.

2.2.4 TPX2 Differentially Inhibits Microtubule Gliding by Eg5 Dimers but Not Monomers

To determine how Eg5-EGFP motors are inhibited by TPX2, microtubule gliding assays using Eg5 dimers and Eg5 monomers were performed. Dimers supported microtubule gliding at an average rate of ~20 nm/s. The velocity of gliding was reduced to ~ 6 nm/s by 250 nM full-length TPX2; the addition of the same concentration of TPX2-710 reduced the velocity of gliding to ~ 15 nm/s, demonstrating that TPX2-710 was a less effective inhibitor than the full-length protein (Fig. 2.5*A*). This result demonstrates that dimeric Eg5 retains the ability to interact with TPX2, consistent with previous *in vitro* binding assays (Ma et al., 2011). In contrast, the velocity of microtubule gliding driven by monomeric Eg5 was inhibited to a similar extent by either full-length or truncated TPX2 (Fig. 2.5*B*). The velocity of microtubule gliding driven by monomeric Eg5 is approximately half the rate of the dimeric construct, presumably due to the uncoordinated action of monomers. Further, these results also show that monomer-driven microtubule gliding is inhibited at lower concentrations of TPX2 or TPX2-710 (Fig. 2.5*B*). For example, the addition of 25 nM TPX2 or TPX2-710 nearly completely halted microtubule gliding by monomeric Eg5, whereas a 20-fold greater concentration of TPX2 is required to result in a similar reduction in the velocity of microtubule gliding by Eg5 dimers. The reason for this increased sensitivity is not known, but it may relate to the presence of a single motor head. These results suggest that the stalk region in the dimeric

construct or the dimer conformation is required for differential inhibition of Eg5 caused by TPX2 and TPX2-710.

2.3 Discussion

2.3.1 Requirements for TPX2 binding to microtubules

The experiments in this chapter shed light on the strength, nature, dynamicity and the requirements of TPX2 binding to the microtubules. The microtubule pelleting experiments show that full length TPX2 binds to microtubules with a high binding affinity of approximately 0.125nM which is consistent with previous observations for *Xenopus* TPX2 (Wittmann et al., 2000) and the affinity falls in the range that is reported for other well characterized microtubule associated proteins like Tau, She1, Map2 and XMAP215 (Makrides et al., 2004; Markus et al., 2012; Illenberger et al., 1996; Brouhardt et al., 2008). Absence of large differences in the binding affinity of full length TPX2 and TPX2-710 suggests that the C-terminal 37 amino acids contributes very little to the microtubule binding ability of TPX2 and the microtubule binding site on TPX2 could be located further upstream.

The single molecule TIRF experiments show that TPX2 and TPX2-710 dynamically binds to microtubules with dwell times of approximately 60sec and that the nature of interaction is electrostatic as the binding of molecules is sensitive to low salt concentrations. Most motor and non-motor microtubule binding proteins bind to microtubules electrostatically by interacting with the highly charged C-terminal region of tubulin called E-hook which is enriched in glutamic acid residues (Wang and Sheetz, 2000; Helenius et al., 2006; Hinrichs et al., 2012). Surprisingly, the experiments with

subtilisin-digested microtubules suggest that TPX2 binding to microtubules does not to involve the highly charged C-terminal E-hook of tubulin. This suggests that TPX2 might bind to regions between adjacent protafilaments unlike most other motor proteins. This is further supported by previous observations where Tau but not TPX2 coated microtubules dissociate from kinesins in a gliding assay (Ma et al., 2011). TPX2 has also been observed to enhance recruitment of E hook binding kinesins Eg5 and Kif15 to the spindle microtubules in cells (Ma et al., 2011; Tannenbaum et al., 2009; Vanneste et al., 2009). This further suggests that the binding site for TPX2 and other E hook binding MAPs may be different which if not would compete off the motors from binding to the microtubules.

2.3.2 Mammalian Cell Extracts as a source of functional Eg5 motors

Previous studies have shown that the biophysical properties of motors obtained from cell extracts are comparable with their purified counterparts (Cai et al., 2007; Gerson-Gurwitz et al., 2011). The experiments in this chapter show that Eg5-EGFP obtained from mammalian cell extracts has many biophysical properties like stepping speed, polarity of walking, ability to bundle and slide antiparallel microtubules and salt sensitivity that are very similar to properties reported for Eg5 EGFP molecules purified from sf9 insect cells (Kapitein et al., 2005; Kwok et al., 2006). Thus mammalian cell extracts could potentially offer a very quick and less arduous way of obtaining highly functional motor proteins for *in vitro* reconstitution experiments that are comparable with the purified versions. By combining the use of cellular extracts with the knockdown-rescue approach in cells, this tool can be very useful to quickly evaluate effects of many things that include post translational modifications, functions of specific domains and the role of interaction partners on motor behavior.

2.3.3 TPX2 regulates Eg5 by Interactions with Both the Motor and Microtubule

The single molecule experiments in this chapter show that Eg5 walking is inhibited by both TPX2 and TPX2-710. This suggests that both TPX2 and TPX2-710 inhibit Eg5 motion on single microtubules by acting as a road block as both TPX2 constructs can bind still to microtubules (Ma et al., 2011). However, the full length TPX2 was a much more potent inhibitor than the truncated TPX2-710. This stronger inhibition suggests that the C-terminal region of TPX2 may enhance the inhibition of Eg5 by promoting its interaction with the motor. Therefore, the inhibition of Eg5 by TPX2 is two pronged mediated both through its ability to bind to microtubule and its ability to directly interact with Eg5. The microtubule gliding experiments (Fig. 2.5D) suggest that the absence of stalk region in Eg5 constructs abolishes the differential inhibition of Eg5 gliding by full length TPX2 and TPX2-710. This suggests that the stalk region may be the target of TPX2 regulation. Elucidating whether the residues in the stalk region is the direct target of physical interaction for TPX2 can be investigated in the future using biochemical assays.

Recent *in vitro* experiments show that TPX2 inhibits the stepping behavior of the kinesin-12, Kif15, the human homolog of Xklp2 (Drechsler et al., 2014). TPX2 enhances the binding of Kif15 to microtubules in pelleting assays and increases its load bearing capacity on microtubules in optical trapping experiments (Drechsler et al., 2014). Though Eg5 is the dominant motor playing a role in the bipolarization of the spindle, Eg5 has been shown to have very short dwell times on spindle microtubules in live cell using TIRF microscopy (Gable et al., 2012). Also, Eg5 has been shown to dissociate from microtubule before stalling in *in vitro* experiments (Korneev et al., 2007) suggesting a

relatively low inherent microtubule affinity under load. Thus, inhibition of Eg5 motion on microtubules by TPX2 may function to increase the residence time of Eg5 on microtubules and potentially enhance its load bearing capacity. In mitotic cells, Eg5 and Kif15 act redundantly to establish and maintain spindle bipolarity and are the predominant plus end directed force generators that balance dynein mediated minus end directed force. Although TPX2 slows Eg5 and Kif15 motion on microtubules, by increasing the force-generating capacity of these motors, it may play a key role in regulating forces needed for spindle bipolarity.

2.3.4 Model for Regulation of Eg5 by TPX2

The data presented here are consistent with the following model for the regulation of Eg5 by TPX2 (Fig. 2.5*C*). Eg5 motors step along the microtubule protofilament and encounter TPX2, resulting in reduced velocity without inducing motor detachment from the microtubule. Results showing that TPX2 does not require the E-hooks for microtubule binding suggest that TPX2 and Eg5 do not compete with each other for microtubule binding. The differential slowing of the motor by full-length and truncated TPX2 demonstrates that binding of TPX2-710 to the microtubule is sufficient to reduce motor velocity but that the C-terminus of TPX2, which interacts with Eg5, results in stronger inhibition (Fig. 2.5*C*). This suggests that TPX2-710 acts as a slowing agent, reducing velocity when encountered by Eg5 motors. Additionally, the data suggest that the C-terminal domain may contribute to the retention of the motor on the microtubule (Ma et al., 2011). Although these experiments and those of others (Drechsler et al., 2014) clearly demonstrate that TPX2 greatly reduces motor stepping on the microtubule, the TPX2-motor interaction must be regulated in live cells so that the motor can generate

sliding forces to establish and maintain spindle bipolarity. Discovering precisely how this MAP-motor interaction is regulated spatially and temporally will provide important insight into spindle function *in vivo*.

2.4 Materials and methods

2.4.1 Materials

All chemicals, unless otherwise specified, were purchased from Sigma-Aldrich.

2.4.2 Cell Culture

LLC-Pk1 cells were cultured in a 1:1 mixture of Ham's F-10 medium and Opti-MEM (Life Technologies, Inc.) containing 7.5% fetal bovine serum and antibiotics at 1X and 5% CO2. Cell extracts were made from LLC-Pk1 cells stably expressing LAP-tagged Eg5 from a bacterial artificial chromosome (Gable et al., 2012).To prepare the extract, a confluent 100-mm diameter cell culture dish was washed twice with 5 ml of room temperature PBS. Then 300 µl of extraction buffer containing 40 mM HEPES/KOH, pH 7.6, 100 mM NaCl, 1 mM EDTA, 1 mM PMSF, 10 µg/ml leupeptin, 1 mg/ml pepstatin, 0.5% Triton X-100, and 1mM ATP (Cai et al., 2007) was added dropwise to the dish and incubated for 2 min without disrupting the monolayer. The cell extract was transferred to a microcentrifuge tube and centrifuged at 14,500 rpm at 4 °C for 10 min in a tabletop centrifuge. The supernatant was recovered and aliquoted into small tubes, flash-frozen, and stored in liquid nitrogen. Protein concentration was determined using the method of Lowry (Lowry et al., 1951). For fluorescent intensity measurement experiments with Eg5- mEmerald, an siRNA-resistant Eg5-mEmerald construct was transiently co-transfected into LLC-Pk1 cells with siRNA directed against endogenous Eg5 (target

sequence CUGAAGACCUGAAGACAAU). The extract was made 48 h post transfection as described. For the extracts used in size exclusion chromatography, cells were not treated with siRNA against endogenous Eg5.

2.4.3 Construction of Plasmids

For bacterial expression, desired nucleotide sequences of human TPX2 constructs (full-length or truncated at amino acid 710) were cloned into a pGEX vector following an N-terminal GST tag and a ULP1 protease cleavage site (Markus et al., 2012). At the C-terminus of TPX2, the stop codon was removed, and the Halo tag sequence was introduced. Constructs were verified by sequencing. For expression in SF9 insect cells, nucleotides coding for full-length human TPX2 or its first 710 amino acids were cloned into the pFast BacAvector after an N-terminal His6 tag, and the constructs were verified by sequencing. The virus for infecting the cells was obtained following the Bac-to-Bac protocol (Invitrogen). The plasmid for monomeric Eg5-367 containing the first 367 amino acids of human Eg5 was a kind gift from the laboratory of Dr. Sarah Rice. The plasmid for the expression of dimeric Eg5-513 containing the first 513 amino acids of Eg5 was a kind gift from the laboratory of Dr. Susan Gilbert.

2.4.4 Protein Purification

Full-length TPX2 and TPX2-710 were expressed and purified from Sf9 cells using the Bac-to-Bac expression system (Invitrogen). Infected cells were harvested, washed with ice-cold water, and resuspended in lysis buffer (50 mM potassium phosphate, pH 8, 250mM KCl, 40mM imidazole, 1% Nonidet P-40, 10 mM β-mercaptoethanol, and a protease inhibitor tablet (Roche Applied Science) on ice. The

lysate was spun at 125,000 X *g* for 45 min at 4 °C. The supernatant was loaded onto pre-equilibrated nickel-nitrilotriacetic acid-agarose beads (Qiagen, Valencia, CA) and incubated for 90 min at 4 °C with end-over-end shaking. The flow-through was removed, and beads were washed with wash buffer (the same as lysis buffer with 10% glycerol and 0.01% Nonidet P-40). The protein was eluted with elution buffer (50mM potassium phosphate, pH 7, 150 mM KCl, 250 mM imidazole, 10% glycerol, 10mM β-mercaptoethanol, and 0.01% Nonidet P-40) and dialyzed in a buffer containing 25 mM HEPES, pH 7.6, 10 mM KCl, 2 mM MgCl2, 10% glycerol, 0.01% Nonidet P-40, and 1 mM DTT for 4 h at 4 °C. Aliquots were flash-frozen in liquid nitrogen and stored at -80 °C. Full-length TPX2-Halo and TPX2–710-Halo were expressed and purified from *Escherichia coli* Rosetta DE3 pLysS cells. In short, 500 ml of culture was grown to an optical density of 0.5–0.8 and induced with 0.1 mM isopropyl 1-thio-D-galactopyranoside at 18 °C for 16 h. The bacteria were harvested and washed with ice-cold distilled water. The cell pellet was resuspended in 2_lysis buffer (60mMHEPES,pH7.4, 0.4mMEGTA, 2 mM DTT, 1.4 _g/ml pepstatin, 1.0 mM Pefabloc, 4 µg/ml leupeptin, and 2 µg/ml aprotinin), diluted to 1X with cold distilled H2O, sonicated on ice (three times for 30 s each at maximum setting), and clarified at 15,000 X *g* for 20 min at 4 °C. The supernatant was incubated for 1 h at 4 °C with glutathione-Sepharose beads that were pre-equilibrated in lysis buffer. The beads were then washed three times in wash buffer (10% glycerol, 300 mM KCl, 0.1% Triton X-100, 1 mM DTT, 0.7 µg/ml pepstatin, and 0.5mM Pefabloc) and twice in TEV buffer (5mM Tris, pH 8.0, 150 mM KCl, 10% glycerol, 0.1% Triton X-100, 1 mM DTT, and 0.5mMPefabloc). The beads were resuspended in TEV buffer and incubated with 23_M Halo tag Alexa Fluor

660 (Promega, Madison, WI) for 15–20 min at room temperature and then washed to remove unbound ligand. The beads were then resuspended in TEV buffer containing Ulp1 protease and incubated at 16 °C for 1 h to cleave protein off of the beads. The supernatant containing the protein was collected by centrifugation, and aliquots were flash-frozen and stored in liquid nitrogen.

Monomeric Eg5-367 was purified from *E. coli* as described (Larson et al., 2010). Briefly, 500 ml of bacteria was grown and induced at an OD of 0.5–0.8 with 0.1 mM isopropyl 1-thio -D-galactopyranoside and incubated at 16 °C for 16 h. The bacteria were pelleted and washed with ice-cold water. The pellet was resuspended in lysis buffer (10mM sodium phosphate buffer, pH 7.2, 20mM NaCl, 2mM MgCl2,1mM EGTA, 1mM DTT, and 0.1mM ATP with protease inhibitor tablet) and lysed by sonication. The lysate was clarified by centrifuging at 15,000X*g* for 30 min at 4 °C. The supernatant was incubated with pre-equilibrated nickel-nitrilotriacetic acid-agarose beads for 90 min at 4 °C. The beads were then washed in wash buffer (same as lysis buffer containing 20mM imidazole) and eluted in elution buffer (same as lysis buffer with 300 mM imidazole). The eluate was then dialyzed against buffer containing 20mM HEPES, pH 7.2, 5mM magnesium acetate, 0.1 mM EDTA, 0.1 mM EGTA, 50 mM potassium acetate, 1 mM DTT, and 5% sucrose for 4 h at 4°C. Aliquots were flash-frozen in liquid nitrogen and stored at -80 °C. Dimeric Eg5-513 was expressed and purified from *E. coli* exactly as described (Ma et al., 2011).

2.4.5 TPX2 Co-sedimentation with Microtubules

Unlabeled tubulin prepared from porcine brains (Hyman et al., 1991) was polymerized and resuspended inPEM100 buffer containing 50μM Taxol. 500 nM full-length TPX2 or TPX2-710 was incubated with indicated concentration of unlabeled polymerized microtubules at room temperature for 10 min. The mixture was centrifuged for 10 min at room temperature in a tabletop centrifuge at maximum speed. The supernatant and pellet fractions were carefully separated. Samples for SDS electrophoresis were prepared by boiling the samples with SDS protein sample buffer and run on an 8% polyacrylamide gel. The proteins were then transferred to a PVDF membrane and probed using antibodies against TPX2 (Novus Biologicals, Littleton, CO) and tubulin (DM1A, Sigma- Aldrich). The blots were developed by chemiluminescence and captured on a Bio-Rad imaging station. Analysis of band intensities were performed using ImageJ. Data were plotted using KaleidaGraph and fit with a quadratic equation (Markus et al., 2012).

2.4.6 TPX2-Halo Microtubule Binding Assays

For TPX2-Halo binding experiments, first 10 _l of 10% rat YL1⁄2 (0.1 mg/ml) anti-tubulin antibody (Accurate Chemical, Westbury, NY) was added to the flow chamber and incubated for 2 min. Second, 0.1 mg/ml rhodamine-labeled microtubules (untreated or treated with subtilisin A) were flowed in and incubated for 2 min. Subtilisin A-treated microtubules were prepared as described (Markus et al., 2012). Third, the surface was blocked by adding 5% Pluronic F-127 and incubated for 2 min. For assays done in epifluorescence, the chamber was incubated with the indicated concentration of

TPX2-Halo for 2 min in PEM 100 (100 mM K-Pipes, pH 6.8, 2 mM MgSO4, and 2mM EGTA) plus 0.5% Pluronic F-127, 50 µM Taxol, 5 mM DTT, 15 mg/ml glucose, 1.23 mg/ml glucose oxidase, and 0.375 mg/ml catalase). Salt (KCl) from a 10X stock of the working concentration was added directly to the buffer. Wide field images were acquired with a constant exposure time. To measure dwell times of TPX2-Halo and TPX2–710-Halo, experiments were performed using TIRF microscopy.

2.4.7 Eg5 Single Molecule Experiments

The concentrations of Eg5 in the extracts were measured by quantitative Western blots. For the single molecule experiments, the perfusion chambers were made from glass slides, silanized coverslips, and double stick tape. 10 µl of 10% rat YL1⁄2 anti-tubulin antibody (Accurate Chemical) was flowed into the chamber and incubated for 3 min. Then the chamber was blocked by flowing in 5% Pluronic F-127 for 3 min. Diluted Cy5-labeled microtubules (composed of a mixture of Cy5 tubulin (Cytoskeleton, Inc., Denver, CO) and unlabeled brain tubulin) were flowed into the chamber and incubated for 3 min, followed by a second block of 5% Pluronic F-127. Eg5 was diluted to 1 or 1.5 nM in motility buffer containing PEM 50 (50mM Pipes, pH 6.9, 2mM EGTA, 2mM MgSO4), 0.5% F-127, 5 mM ATP, 1 mM DTT, 25 µM Taxol supplemented with an oxygen-scavenging system (15 mg/ml glucose, 1.23 mg/ml glucose oxidase, and 0.375 mg/ml catalase) and flowed into the chamber and imaged. For preincubation experiments with TPX2, the indicated concentrations of TPX2 were added to the motility buffer along with Eg5 in extract and incubated on ice for 2 min before flowing into the chamber.

2.4.8 Kinesin-1 Single Molecule Experiments

Perfusion chambers were made as described above. 10µl of 10% rat YL1⁄2 anti-tubulin antibody, 5% Pluronic F-127, and diluted Cy5-labeled microtubules were added sequentially and incubated for 5 min each. The chamber was washed with PEM100 plus Taxol. Kinesin-1 was diluted in PEM 100 with 10 mM DTT. This was then added to the motility buffer (PEM 100, 25 µM Taxol, 0.5% Pluronic F-127, 0.5 mg/ml BSA, oxygen-scavenging system, and 0.5 mM ATP) and flowed into the chamber and imaged. For experiments with TPX2 addition, TPX2-Halo was diluted into the motility buffer (without kinesin-1) and flowed into the chamber during image acquisition.

2.4.9 Microtubule-Microtubule Gliding Assays

Biotinylated, Cy5- labeled microtubules were immobilized on silanized coverslips using anti-biotin antibody (Sigma-Aldrich). The chamber was blocked using 5% Pluronic F-127. Eg5-EGFP from extracts was preincubated with rhodamine-labeled microtubules for 3 min, and the mixture was flowed into the chamber. Finally, motility buffer was added, followed by acquisition on a TIRF microscope.

2.4.10 Size Exclusion Chromatography

Eg5-EGFP was purified from SF9 insect cells as per the manufacturer's instructions (Bac to Bac, Invitrogen). The extract from LLC-Pk1 cells was prepared as mentioned before. The Superose 6 10/300 GL column (GE Healthcare) was pre-equilibrated with 10mM HEPES, pH 7.6, 0.05% Triton X-100, 100 mM NaCl, 1 mM ATP before use. 100 µl of the purified protein was loaded onto the column and run at a constant flow rate of 0.2 ml/min. The elution profile of Eg5-EGFP was directly followed

by measuring absorbance at 488 nm. For the size exclusion of LLC-Pk1 cell extracts, 175 µl of cell extract was loaded on the column and run under identical conditions. The collected fractions were separated by SDS-PAGE, transferred to a PVDF membrane, and probed for the presence of Eg5 using Western blot.

2.4.11 Microtubule Surface Gliding Assays

Perfusion chambers of 10 µl in volume were made using glass slides and coverslips with a double stick tape spacer. For gliding assays with the Eg5-367 monomer, the chamber was incubated with anti-His antibody and 2 mg/ml BSA for 3 min, followed by two washes with motility buffer (80 mM PIPES, pH 6.8, 2 mM MgCl2, 1 mM EGTA, 0.2 mg/ml BSA, and 150 mM sucrose). Then the chamber was incubated with Eg5-367 for 3 min and washed again with motility buffer. Finally, the activation mix, consisting of motility buffer containing oxygen-scavenging system, ATP, Taxol, and diluted Cy5-labeled microtubules was added and imaged on a Nikon TiE microscope using epifluorescence. Surface gliding experiments with the dimeric Eg5-513 were performed exactly as described by Ma *et al.* (Ma et al., 2011). For the TPX2 addition experiments, the TPX2 constructs were added to the activation mix, incubated for 2 min on ice, and then flowed into the chamber.

2.4.12 Microscope Imaging and Analysis

TIRF microscopy was performed using a microscope (Ti-E; Nikon Instruments, Melville, NY) equipped with a 60X, 1.4 numerical aperture objective lens. The system was run by Elements software (Nikon Instruments). Images were acquired using a 512 X 512-pixel camera (Cascade II; Photometrics, Tuscon, AZ). A _4 image expansion

telescope in front of the camera was used. The nm/pixel ratio was 68.5 nm/pixel. A blue diode laser (488 nm, 50 milliwatts) was used. Images were acquired every 2 or 3 s for 10 min. For two-color TIRF, a 488-nm argon laser and a 647-nm diode laser were used on a custom-built TIRF system on a Nikon TiE stand, run by Elements software. A 60X objective lens was used; exposure times for both red and green illumination were 50 –100 ms. Wide field imaging for Eg5-513 gliding assays and for binding of TPX2- Halo to microtubules was performed using epifluorescence illumination.

2.4.13 Quantification of Gliding Velocity, Single Molecule Velocity, and MSD

The velocity of Eg5-513- and Eg5-367-dependent microtubule gliding movement was calculated using the MTrackJ plugin in ImageJ. To calculate the velocity of Eg5-EGFP single molecules from TIRF images, ImageJ was used to generate a kymograph of moving molecules. Velocities were calculated by manually tracking individual puncta. The data were ported to Excel, and a polynomial 2 trend line was added to the MSD *versus* time plot to determine the diffusion coefficient (*D*).

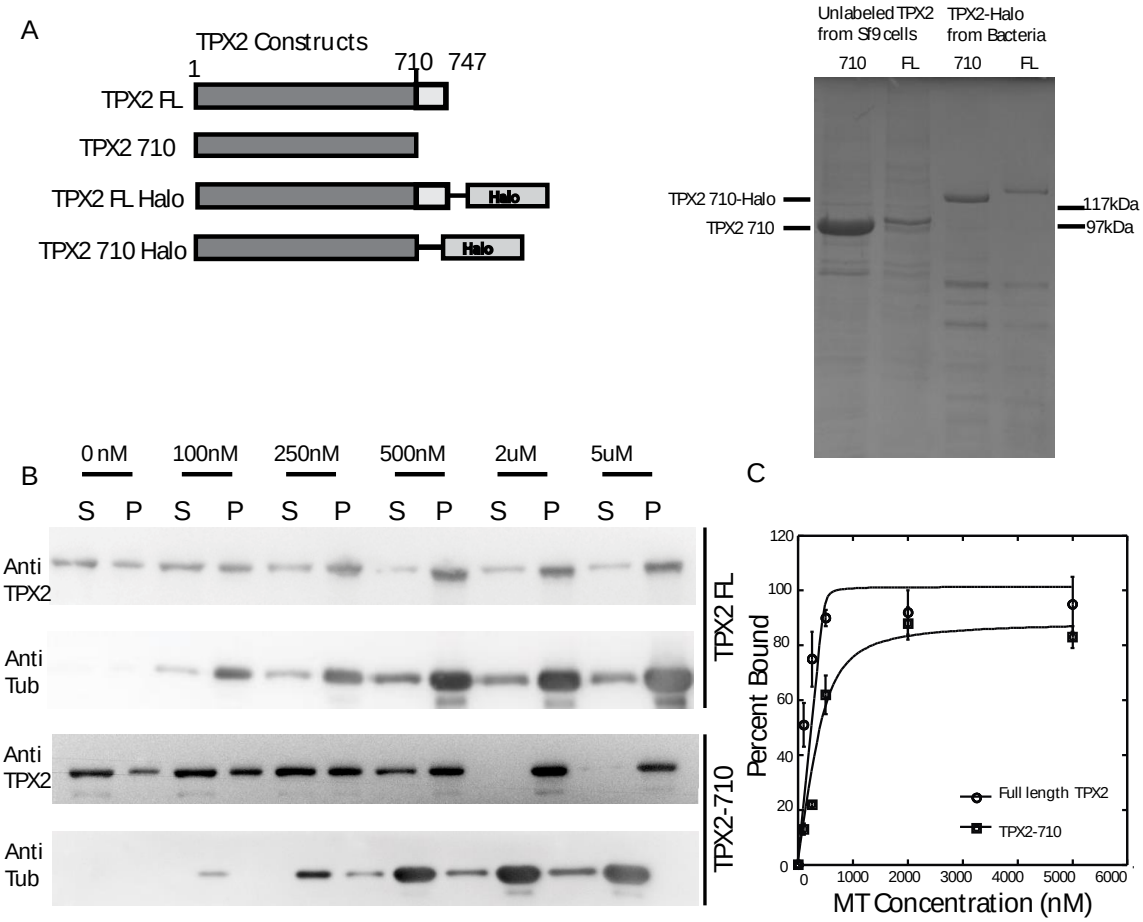

Figure 2.1 Binding of TPX2 and TPX2-710 to microtubules. (*A)* schematic diagram of the TPX2 constructs (*left*) and Coomassie Brilliant Blue-stained gel of the purified proteins (*right*). (*B*) co-sedimentation of TPX2 with microtubules. *S*, supernatant; *P*, pellet. The concentration of microtubules in each *pair* of *lanes* is noted *above*. Western blots were stained for TPX2 or tubulin. (*C*) quantification of apparent affinity was performed using a quadratic fit. The experiment was performed twice, and the values were averaged. *Error bars*, S.D.

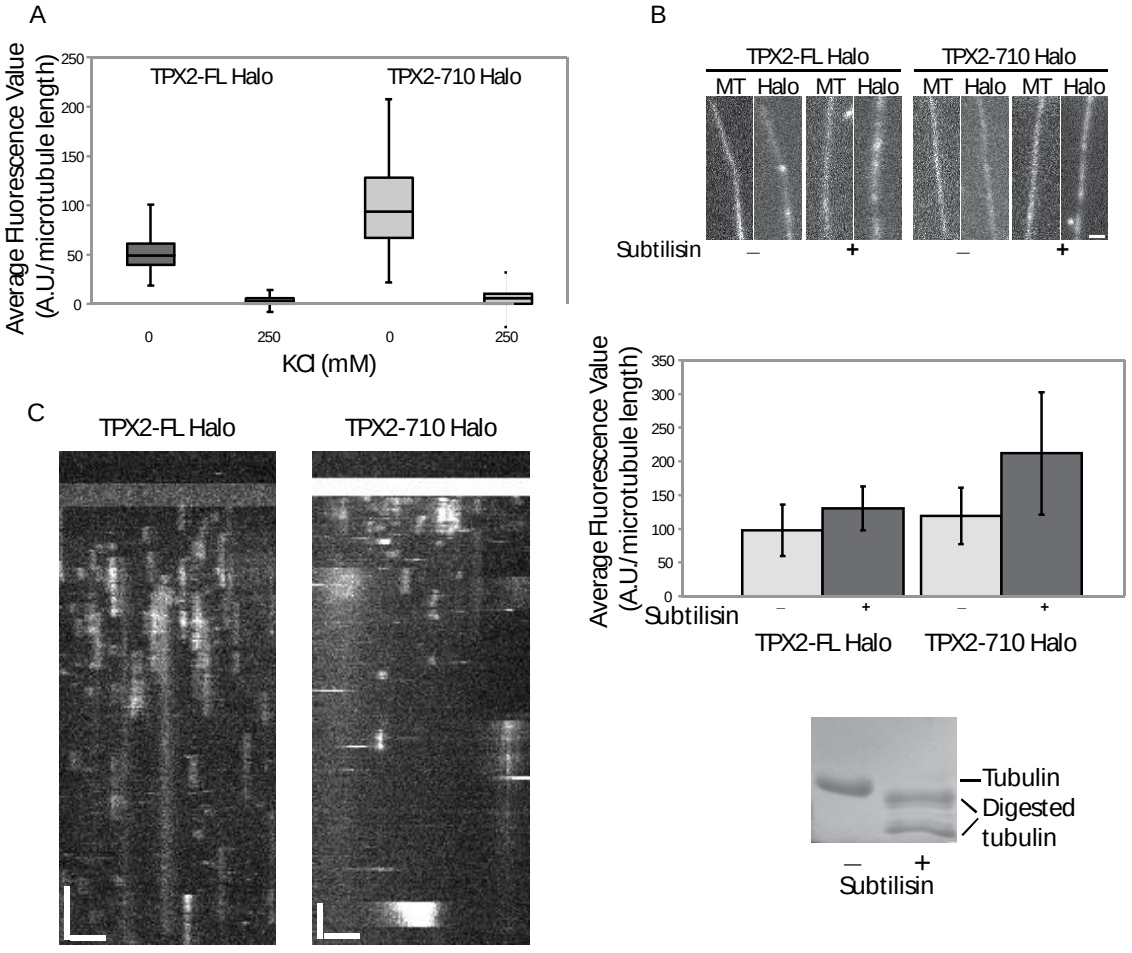

Figure 2.2 Binding Dynamics of TPX2 and TPX2-710. (*A*) box plot showing release of TPX2 and TPX2–710 from microtubules in the presence of the indicated concentration of KCl added to the buffer. TPX2 fluorescence is reported as arbitrary units (*A.U.*). *Whiskers* define the range, *boxes* encompass the 25th to 75th quartiles, and *lines* depict the medians. (*B*) TPX2 and TPX2-710 binding to untreated and subtilisin A-digested microtubules; *top panels*, fluorescence images of TPX2-Halo or TPX2–710-Halo bound to untreated and subtilisin A-digested microtubules; *middle*, quantification of TPX2 fluorescence; *bottom*, polyacrylamide gel showing digested and control microtubules. TPX2 fluorescence was measured for at least 60 microtubules for each of two independent experiments; *error bars*, S.D. (*C*) kymograph of TPX2-Halo and TPX2-710-Halo on microtubules. *Vertical scale bar* (time), 60 s; *horizontal scale bar*, 2 µm.

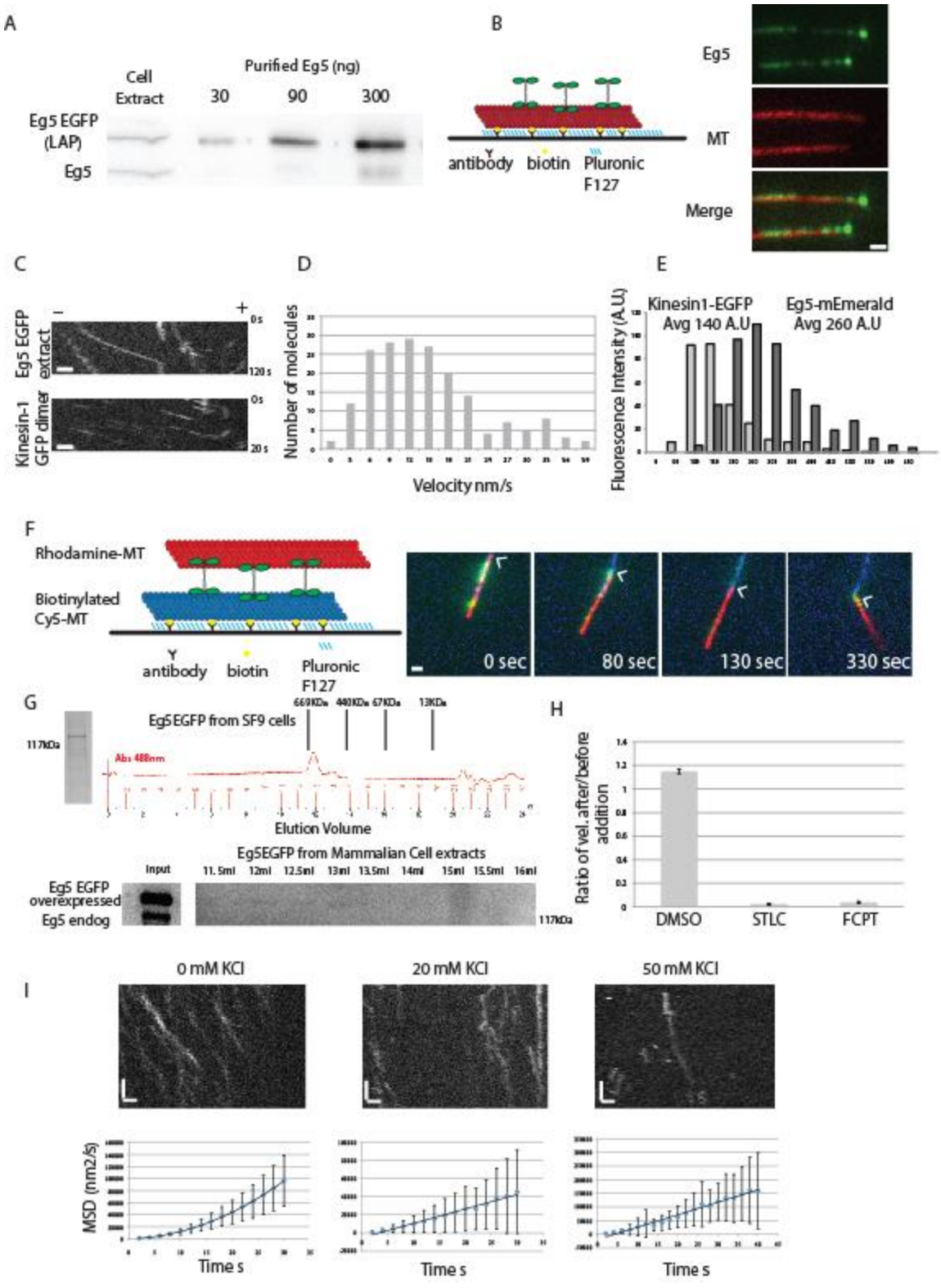
A
Cell Extract
Purified Eg5 (ng)
30
90
300
Eg5 EGFP (LAP)
Eg5
B
antibody
biotin
Pluronic F127
Eg5
MT
Merge
C
Eg5 EGFP extract
Kinesin-1 GFP dimer
0s
120 s
20 s
D
Number of molecules
Velocity nm/s
E
Kinesin1-EGFP Avg 140 A.U
Eg5-mEmerald Avg 260 A.U
Fluorescence Intensity (A.U.)
F
Rhodamine-MT
Biotinylated Cy5-MT
antibody
biotin
Pluronic F127
0 sec
80 sec
130 sec
330 sec
G
Eg5EGFP from SF9 cells
669KDa
440KDa
67KDa
13KDa
117kDa
Abs 488nm
Elution Volume
Eg5EGFP from Mammalian Cell extracts
Input
11.5ml
12ml
12.5ml
13ml
13.5ml
14ml
15ml
15.5ml
16ml
Eg5 EGFP overexpressed
Eg5 endog
117kDa
H
Ratio of vel. after/before addition
DMSO
STLC
FCPT
I
0 mM KCl
20 mM KCl
50 mM KCl
MSD (nm2/s)
Time s
Time s
Time s

Figure 2.3 Characterization of Eg5 in mammalian cell extracts. (*A*) Western blot of cell extract and purified Eg5. (*B*) schematic diagram of the single molecule TIRF experiments (*left*) and TIRF images of Eg5-EGFP accumulating at the microtubule plus-end (*right*). (*C*) kymographs of kinesin-1 EGFP dimers and Eg5-EGFP from extracts on the same microtubule. Note the different time scale. Plus- and minus-ends of the microtubules are indicated. (*D*) histogram of Eg5-EGFP motor velocity. (*E*) histogram of the fluorescence of kinesin-1 dimers (*light gray*) and Eg5 molecules (*dark gray*) in the extract. (*F*) schematic diagram (*left*) and fluorescence images (*right*) showing microtubule-microtubule sliding by Eg5. The *arrowhead* marks the end of the sliding microtubule. (*G*) Coomassie Brilliant Blue-stained gel of Eg5-EGFP purified from insect cells and the trace of absorbance at 488nmon the size exclusion column for the purified protein. The Western blot shown is for the fractions obtained from size exclusion chromatography of Eg5-mEmerald from LLC-Pk1 extract probed for Eg5. (*H*) quantification of the velocity of Eg5-EGFP after the addition of DMSO, STLC, or FCPT (*right*). *Error bars*, S.E. (*I*) directional and diffusive motility of Eg5-EGFP in the presence of 0, 20, or 50mMKCl added to the motility buffer. *Top*, kymographs; *bottom*, mean squared displacement. *Horizontal scale bar* (*B*, *C*, *F*, and *I*), 1µm; *vertical scale bar* (*I*), 60 s. *Vertical scale* in (*C)* is shown on the image. *A.U.*, arbitrary units.

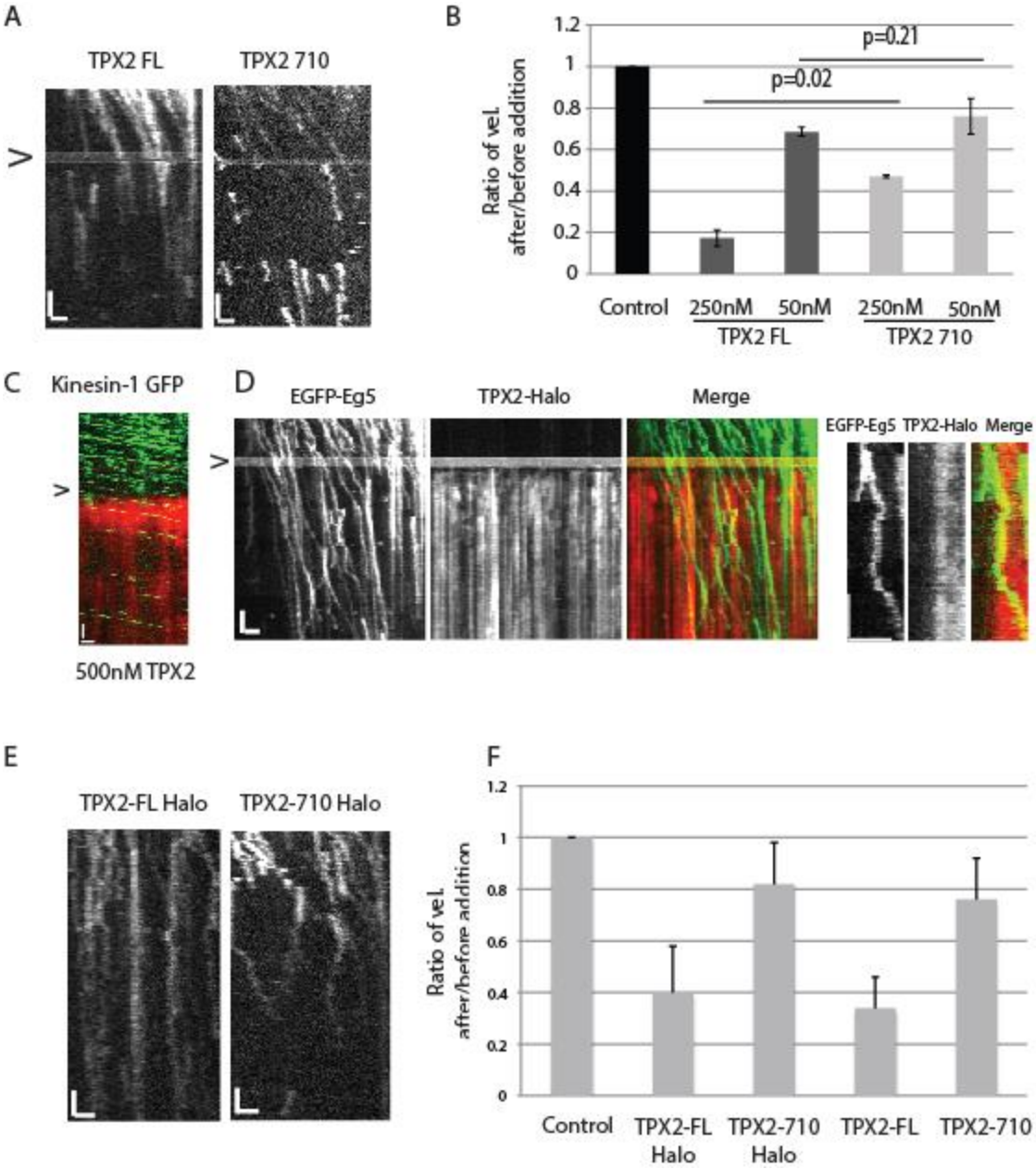

Figure 2.4 Inhibition of Eg5 by TPX2 requires both binding to the microtubule and an interaction between TPX2 and Eg5. (*A)* kymographs of Eg5-EGFP before and following the addition ofTPX2or TPX2–710; *arrowhead*, time of theTPX2addition.(*B)* quantification of Eg5-EGFP velocity; *error bars*, S.D.(*C*) kymographof kinesin-1EGFP dimers walking on microtubules before and after the addition of TPX2 (*arrowhead*). 1 nM kinesin-1 EGFP (*green*) and 500 nM TPX2-Halo (*red*) were used. (*D*) kymographs of Eg5-EGFP (*green*) before and following the addition of 20 nM TPX2-Halo (*red*). *Right panels*, enlarged view. (*E*) kymographs of Eg5-EGFP that was premixed with TPX2-Halo or TPX2–710-Halo. (*F*) quantification of Eg5-EGFP velocity in the presence of 50 nMTPX2 that was Halo-tagged (*left*) or untagged (*right*). *Errorbars*, S.E. *Horizontal scale bars* (*A*, *C*, and *E*), 1μm; *horizontal scale bar* (*D*), 2μm; *vertical scale bar*, 60 s (*A*, *D*, and *E*) and 5 s (*C*).

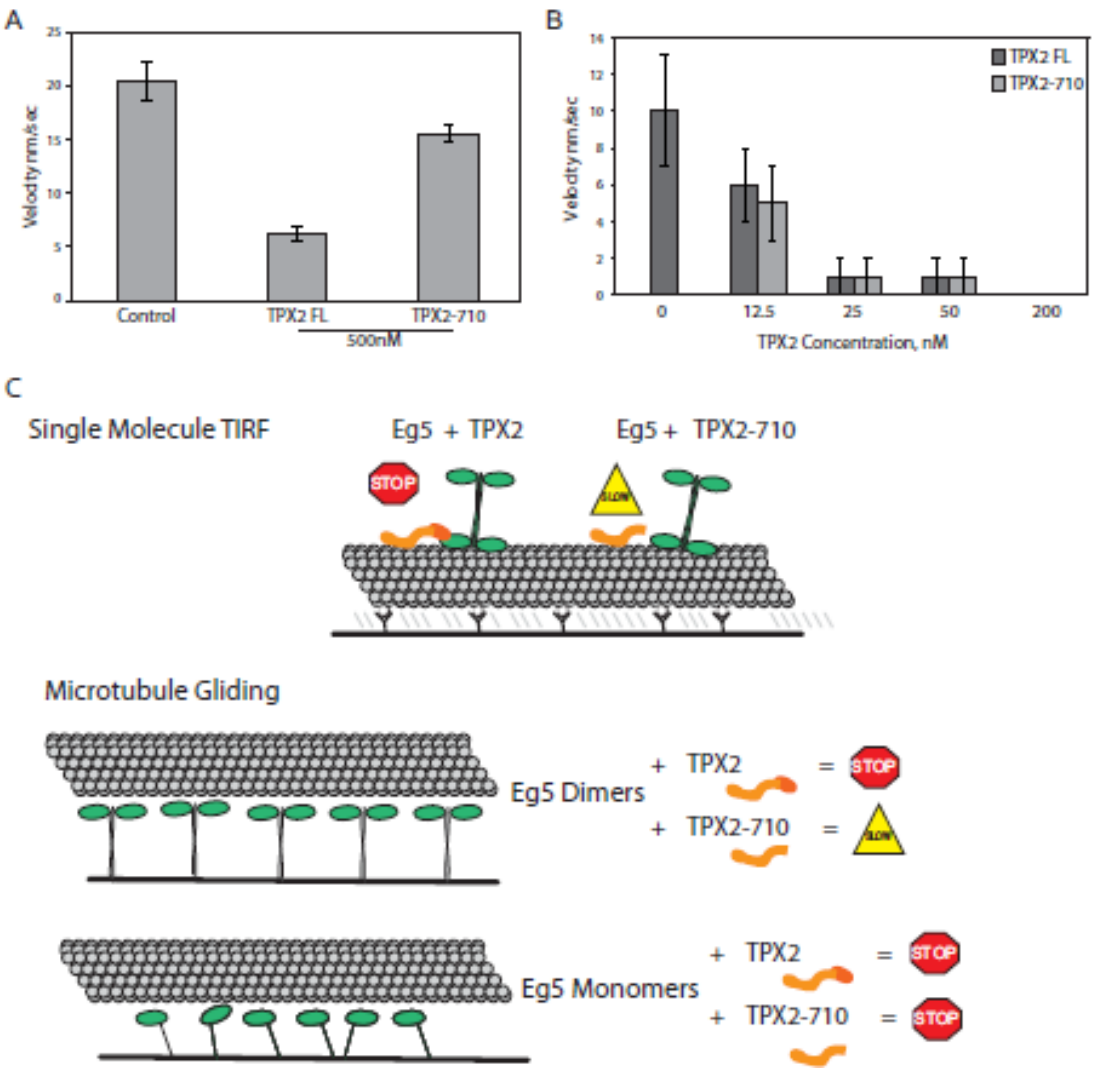

Figure 2.5 Differential regulation of Eg5 dimers, but not monomers, by full-length and truncated TPX2. Shown is velocity of microtubule gliding driven by Eg5 dimers (*A*) or Eg5 monomers (*B*). *Error bars*, S.E. *C*, model for inhibition of Eg5 by TPX2. *Top*, inhibition of motor stepping by full-length (*left*, *stop symbol*) and truncated TPX2 (*right*, *slow symbol*) in single molecule assays. *Bottom panels*, inhibition of microtubule gliding by Eg5 dimers (*top*) and Eg5 monomers (*bottom*). *Green*, Eg5; *orange*, TPX2.

CHAPTER 3

REGULATION OF KIF15 LOCALIZATION AND MOTILITY BY C-TERMINUS OF TPX2 AND MICROTUBULE DYNAMICS

The TPX2 constructs used in the single molecule experiments were purified from Bacteria by Barbara J Mann. The Kif15 single molecule experiments and data analysis presented in this chapter were performed in collaboration with Barbara J Mann.

3.1 Introduction

During mitosis, microtubules are nucleated and organized into a dynamic structure called the mitotic spindle, which mediates chromosome segregation into two daughter cells. In mammalian cells, microtubule nucleation at centrosomes, near chromatin, and from preexisting microtubules all contribute to spindle formation (Meunier and Vernos, 2016). Microtubule formation near chromatin and at kinetochores is regulated by nuclear localization sequence containing spindle assembly factors that are inactive when bound to importins α/β (Gruss and Vernos, 2004). The small GTPase Ran, which is locally activated near chromatin (Kalab et al., 2006), binds to importin β and relieves this inhibitory effect, thus promoting microtubule formation. A well-studied Ran-regulated spindle assembly factor is TPX2, which stimulates microtubule formation at kinetochores and in the chromatin region and is required for spindle assembly and completion of mitosis (Tulu et al., 2006; O'Connell et al., 2009).

During spindle formation the duplicated centrosomes separate to establish spindle bipolarity. Centrosome separation is driven by the kinesin-5, Eg5, a bipolar, tetrameric motor that cross-links and slides antiparallel microtubules (Kapitein et al., 2005; Ferenz et al., 2010). More recently, it was shown that after bipolar spindle formation, the action of Eg5 is dispensable, and spindle bipolarity is maintained by a kinesin-12, Kif15 (Tanenbaum et al., 2009; Vanneste et al., 2009). Spindles in cells depleted of Kif15 are shorter than spindles in control cells, consistent with a model in which Kif15, like Eg5, generates outward force in the spindle (Sturgill and Ohi, 2013). However, in contrast to Eg5, Kif15 preferentially associates with kinetochore fiber microtubules. Cells overexpressing Kif15 can form a bipolar spindle in the absence of Eg5 activity (Tanenbaum et al., 2009; Raaijmakers et al., 2012; Sturgill and Ohi, 2013). The existence of two mitotic motors that can each power bipolar spindle formation may contribute to the lack of efficacy of Eg5 inhibitors in clinical trials, and understanding how these motors are regulated therefore may be of clinical significance (Waitzman and Rice, 2014).

Localization of kinesin-12 and kinesin-5 motors to spindle microtubules requires TPX2 (Tanenbaum et al., 2009; Vanneste et al., 2009; Ma et al., 2011). In fact, TPX2 was initially discovered as a factor required for the dynein-dependent targeting of the *Xenopus* kinesin-12, Xklp2, to spindle poles (Wittmann et al., 1998). The C-terminal 37 amino acids of TPX2 are required to target Eg5 to the spindle; targeting of Kif15 requires the C-terminal leucine zipper of the motor (Wittmann et al., 1998). The C-terminal half of TPX2 is required to localize Kif15 to the spindle (Brunet et al., 2004), but it was not known whether a specific domain of the protein is necessary.

These initial studies on TPX2 and Kif15 were consistent with the idea that dimers of Kif15 walked along one microtubule while tethered to a second microtubule via TPX2, thus generating force for spindle formation (Vanneste et al., 2009).

Subsequently Sturgill et al. (2014) provided biochemical data showing that the motor was an autoinhibited dimer and identified a second, nonmotor microtubule-binding site in the coil 1 region of Kif15. These data led to a model in which autoinhibited Kif15 dimers were first unmasked and then bound to microtubule bundles via motor and nonmotor binding sites (Sturgill et al., 2014). More recent work, however, showed that Kif15 exists as a tetramer that displays processive motility along individual microtubules in vitro (Drechsler et al., 2014; Drechsler and McAinsh, 2016). Thus the oligomeric state of Kif15 and how it contributes to mitotic spindle formation remain unresolved. Finally, experiments using dynamic microtubules in vitro show that Kif15 accumulates at microtubule plus ends, suppresses catastrophe events, and can cross-link microtubules and move them relative to one another, promoting the formation of parallel microtubule arrays (Drechsler and McAinsh, 2016). Thus both Eg5 and Kif15 contribute to spindle bipolarity and are regulated by TPX2, but their mechanisms of action are distinct.

To gain insight into the cellular function and regulation of the kinesin-12, Kif15, the experiments in this chapter investigate the behavior of the motor and its regulation by TPX2 in vitro and in vivo. The results presented here show that Kif15 motors, present in diluted mammalian cell extracts, are processive, track-switching tetramers and that the C-terminal region of TPX2 is required to inhibit Kif15 motor stepping. Using a knockdown-rescue approach in mammalian cells the C-terminal region of TPX2 was determined to contribute to targeting of the motor to the mitotic spindle and that Eg5-independent

bipolar spindle formation by overexpressed Kif15 requires the TPX2 C-terminal region. In live cells, GFP-Kif15 display robust, plus end–directed motility at a rate similar to that of microtubule growth, and this behavior is suppressed by paclitaxel. Together these results document the behavior of Kif15 in cells and demonstrate the importance of TPX2 and its C-terminal region for motor localization and activity.

3.2 Results

3.2.1 TPX2 C-terminus contributes to Kif15 targeting to spindle microtubules

The C-terminal 37 amino acids of TPX2 contribute to the targeting of the kinesin-5, Eg5, to spindle microtubules (Ma et al., 2011), but it is not known whether this domain contributes to the targeting of the kinesin-12, Kif15, to the spindle (Wittmann et al., 1998; Brunet et al., 2004; Tanenbaum et al., 2009; Vanneste et al., 2009). To address this, the distribution of endogenous Kif15 was examined in LLC-Pk1 cells expressing full-length TPX2 or TPX2-710, which lacks the C-terminal 37 amino acids, from bacterial artificial chromosomes (BACs) and depleted of the endogenous protein using small interfering RNA (siRNA; Ma et al., 2011). Cells were fixed and stained for microtubules and Kif15 at 40 h after nucleofection with TPX2 siRNA, a time when the majority of TPX2 is depleted (Ma et al., 2011). Kif15 was present along spindle microtubules in parental LLC-Pk1 cells but not in parental cells depleted of TPX2 (Fig 3.1A). In LLC-Pk1 cells expressing full-length TPX2 or TPX2-710 from a BAC and depleted of endogenous TPX2, Kif15 was detected on spindle microtubules when full-length TPX2 was present and was reduced when TPX2-710 was expressed (Fig 3.1A). Quantification of the ratio of Kif15 to microtubules at the spindle pole and in the spindle midway

between the chromosomes and pole shows a statistically significant reduction at both locations in cells expressing TPX2-710 compared with cells expressing full-length TPX2 (Fig 3.1C). As previously reported (Ma et al., 2011), expression of TPX2-710 in cells depleted of TPX2 resulted in aberrant spindle morphology (Fig 3.1B). These results demonstrate that for both Eg5 and Kif15, the C-terminal domain of TPX2 contributes to spindle targeting.

A recent study has shown that the kinase Aurora A dependent phosphorylation of Kif15 in the tail fragment enhances the recruitment of Kif15 on the spindle microtubules (van Heesbeen et al., 2016). As TPX2 has been shown to activate the kinase Aurora A, TPX2 C terminus dependent spindle localization of Kif15 could be mediated through the activation of the kinase. To test this, control or siTPX2 treated TPX2-FL and TPX2-710 BAC cells were fixed and stained for microtubules and phosphorylated Aurora A. Even in the absence of endogenous TPX2, phosphorylated Aurora staining was observed in both the TPX2-FL and TPX2-710 BAC cells suggesting that Aurora A activation is not compromised in these cells (Fig 3.2). This is consistent with previous studies that indicate that the N terminal residues of TPX2 bind and activate Aurora A (Kufer et al., 2002; Eyers and Maller, 2004). As a negative control, when the cells are treated with Aurora A inhibitor MLN8236, the phosphorylated Aurora A staining is diminished (Fig 3.2). These results suggest that the TPX2 C terminus dependent spindle localization of Kif15 may not be mediated through Aurora A activation and may depend on other functions of TPX2.

3.2.2 Full-length TPX2 inhibits Kif15 motor velocity

Next, the requirement of whether C-terminal domain of TPX2 was required to regulate Kif15 motor stepping *in vitro* was determined. To do this, LLC-Pk1 cells was transfected with full-length Kif15 tagged with enhanced green fluorescent protein (GFP-Kif15; Vanneste et al., 2009) and a stable cell line was generated. These cells were used to prepare cytoplasmic extracts for use in single-molecule total internal reflection fluorescence (TIRF) microscopy experiments (Fig 3.3A; Cai et al., 2007; Balchand et al., 2015). Rhodamine-labeled, paclitaxel-stabilized microtubules were attached to the surface of a microscope flow chamber, and cell extract diluted in motility buffer was added. Fluorescent puncta were observed to bind to microtubules and processively move upon addition of ATP (Fig 3.3, A, B, and F). Of note, nearly every GFP-Kif15 puncta that bound a microtubule was motile, demonstrating that Kif15 from mammalian cells is not autoinhibited (Sturgill et al., 2014) but displays robust motility. TPX2 is undetectable in these cytoplasmic extracts because they are prepared from asynchronous cells, >95% of which are in interphase, a time when TPX2 is located in the nucleus (Balchand et al., 2015).

GFP-Kif15 was observed to move predominantly in a plus end–directed manner (86% of events), with a smaller percentage of events toward the minus end (14% of events; Drechsler et al., 2014; Fig 3.3A). The average velocity of plus end–directed motion was 128.7 nm/s, and the velocity of minus end–directed motion was slower, 86.6 nm/s. Motility was processive, with average run lengths of 1.9 and 0.9 μm in the plus- and minus-end directions, respectively (Fig 3.3A). In addition to directional reversals, Kif15 motors moving on one microtubule could switch to a neighboring microtubule and

continue processive motility (Fig 3.3B). In extracts prepared from LLC-Pk1 cells arrested in mitosis with a low concentration of nocodazole (Materials and Methods), motor velocity (151 nm/s, n = 54, 53 plus-end directed and 1 minus-end directed) was not different from that measured in interphase, with the caveat that TPX2 is present in these extracts. Of interest, minus end–directed motility was reduced in the mitotic compared with the interphase extract. These data suggest that in *in vitro* assays, motor microtubule affinity is sufficiently strong to overcome any potential mitotic regulation (vanHeesbeen et al., 2016). This possibility is consistent with the observation that Eg5 prepared from interphase extracts, and thus lacking the mitosis-specific phosphorylation required for its spindle microtubule binding (Blangy et al., 1995), shows robust motility in vitro (Balchand et al., 2015).

Kif15 was previously reported to exist as a tetramer or dimer using purified motors (Drechsler et al., 2014; Sturgill et al., 2014) or motors in mammalian cell extracts (Drechsler and McAinsh, 2016; Sturgill et al., 2016). Understanding the quaternary structure of the molecule is significant because tetramers can potentially interact with more than one microtubule simultaneously and formation of tetramers could potentially alter the availability of a second microtubule-binding site in the motor tail (Sturgill et al., 2014). To determine the oligomeric state of GFP-Kif15 in our experiments, images of purified kinesin-1-GFP, which is known to be a dimer, and GFP-Kif15 using identical imaging conditions were acquired using only motors that bound to microtubules. For this experiment, endogenous Kif15 was depleted from the cells before preparation of the extract, so that the motors would be composed predominantly of the expressed GFP-tagged protein. As shown in the histogram in Fig 3.3C, (bottom), Kif15 puncta showed a

range of fluorescence intensities, with an average intensity that was 1.6 times the average fluorescence intensity of kinesin-1–GFP (Fig 3.3C, top; average fluorescence of 220.5 and 141.0 arbitrary units). The reason that the average value was not twice the intensity of kinesin-1-GFP may result from incomplete depletion of endogenous Kif15 by siRNA, resulting in a mixture of motors containing two, three, or four GFP-tagged motors. In addition, some motors may dissociate into dimers during preparation (Drechsler et al., 2014; Sturgill et al., 2014, 2016). To determine whether Kif15 exists as a tetramer, cell extract was added to microtubules in chambers without ATP and the number of bleach steps was counted. In this experiment, more than half the particles observed displayed greater than three bleach steps (Fig 3.3D), demonstrating that in cell extracts, some of the Kif15 motors exist as tetramers.

In summary, these data show that GFP-Kif15, prepared from mammalian cells, moves rapidly and processively toward microtubule plus ends and can both switch microtubule tracks and reverse direction. The motile parameters of Kif15 prepared from mammalian cells are strikingly similar to motors purified from Sf9 cells and indicate that the native state of Kif15 in interphase and mitotic mammalian cells is likely a tetramer (Drechsler et al., 2014) that can dissociate into dimers depending on the experimental conditions (Drechsler et al., 2014; Drechsler and McAinsh, 2016; Sturgill et al., 2014, 2016).

To identify the region, or regions, of TPX2 that regulate Kif15 motility in vitro, different TPX2 constructs were incubated with diluted extract containing GFP-Kif15 and then introduced it into the motility chamber. When full-length TPX2 was present in the reaction, motor velocity was reduced to ~65% of controls (Fig 3.3, E and F). Next,

TPX2-710 which binds microtubules (Balchand et al., 2015) and contributes to motor targeting was added (Fig 3.1) to determine whether it also regulates motility *in vitro*. Incubation of TPX2-710 with GFP-Kif15 before addition to the motility chamber did not result in a statistically significant reduction in motor velocity (Fig 3.3 E and F) demonstrating that full-length TPX2 is required for motor inhibition. Two additional constructs, one lacking a larger C-terminal region (TPX2-657) and one containing a deletion of a conserved PFAM domain near the C-terminus (TPX2-ΔPFAM), also failed to inhibit Kif15 (Fig 3.3 E and F). The lack of inhibition with the ΔPFAM construct, which is missing only part of the region deleted in TPX2-710, indicates that these nine amino acids may play a role in motor inhibition. Both TPX2-657 and TPX2-ΔPFAM bound microtubules after expression in mammalian cells depleted of endogenous TPX2 (Data not shown), demonstrating that failure to inhibit Kif15 did not result from failure of these proteins to bind microtubules. In summary, these experiments show that full-length TPX2 is required to inhibit Kif15 motor stepping in vitro.

3.2.3 TPX2 is required for bipolar spindle formation in cells overexpressing Kif15

Previous work showed that bipolar spindle formation can proceed in cells lacking Eg5 activity and overexpressing Kif15, demonstrating that Kif15 can generate force for spindle formation *in vivo* (Tanenbaum et al., 2009; Sturgill and Ohi, 2013). To understand how TPX2 contributes to Kif15-dependent spindle formation in vivo, spindle formation in LLC-Pk1 cells overexpressing GFP-Kif15 was examined. In these cells, the distribution of GFP-Kif15 on spindle microtubules was similar to the distribution of Kif15 in the parental cells, showing a punctate staining pattern with enrichment along kinetochore fiber microtubules and near spindle poles (Fig 3.4A). This distribution is

equivalent to that observed in *Xenopus* cultured cell spindles (Wittmann et al., 2000) and similar to the distribution in other cultured mammalian cells (Tanenbaum et al., 2009; Vanneste et al., 2009; Sturgill and Ohi, 2013). Western blots of an extract of GFP-Kif15 cells show that GFP-Kif15 is present at approximately 10 times the level of endogenous Kif15 in the parental cells (Fig 3.4B).

Treatment with siRNA targeting TPX2 resulted in a dramatic reduction in GFP-Kif15 on spindle microtubules and an ensuing increase in the level of cytoplasmic fluorescence (Fig 3.4C). In some cells, residual GFP-Kif15 was detected near spindle poles (Fig 3.4C). These results demonstrate that TPX2 contributes to the localization of GFP-Kif15 to spindle microtubules, even when high levels of the motor are present.

In control cells, Kif15 is enriched on kinetochore fiber microtubules (Sturgill and Ohi, 2013) and when overexpressed, Kif15 binds and stabilizes nonkinetochore microtubules as well, where it is believed to play a key role in Eg5-independent spindle formation (Sturgill and Ohi, 2013). In cells depleted of Nuf2, a treatment that prevents kinetochore fiber formation, GFP-Kif15 remained associated with the spindle (Fig 3.4C, left) despite the loss of kinetochore fibers and concomitant failure of chromosome congression (Fig 3.4C, right). Then the requirement for kinetochore fibers for Kif15 spindle localization was tested in parental cells by depleting Nuf2 and staining for Kif15 (unpublished data); in these cells, the spindle localization of Kif15 is reduced but not completely abolished, consistent with previous observations (Vanneste et al., 2009). Together these results show that overexpressed GFP-Kif15 is distributed in a manner similar to that of the endogenous protein and that TPX2, but not kinetochore fibers, is required for spindle localization.

To examine Kif15-dependent spindle formation in LLC-Pk1 GFP-Kif15 cells, parental and GFP-Kif15 cells were treated with 1 μM S-trityl-L-cysteine (STLC; DeBonis et al., 2004) for 18 h and spindle morphology was quantified (Fig 3.4D). In parental cells treated with STLC, 96% of spindles were monopolar. In STLC-treated GFP-Kif15 cells, the majority of spindles were bipolar (87%), demonstrating that GFP-Kif15 can support bipolar spindle formation in these cells, consistent with results in other mammalian cells either overexpressing Kif15 or treated to develop resistance to STLC (Vanneste et al., 2009; Raaijmakers et al., 2012; Sturgill and Ohi, 2013; Sturgill et al., 2016). Next, the ability of STLC-treated, GFP-Kif15–expressing cells to form bipolar spindles after siRNA-mediated depletion of TPX2 was assessed. 97% of spindles were monopolar (Fig 3.4D), indicating that TPX2 is required for Kif15-dependent bipolar spindle formation (Tanenbaum et al., 2009). It should be noted, however, that depletion of TPX2 in control cells also leads to defects in spindle formation, resulting in short bipolar spindles, multipolar spindles, and monopolar spindles (Gruss and Vernos, 2004)

As previous results in this chapter showed that the C-terminal 37 amino acids of TPX2 are important for spindle localization of Kif15 and inhibition of Kif15 motility in vitro, cell lines expressing full-length or truncated TPX2-710 from a BAC were next used to determine whether the C-terminal region is important for force generation by Kif15 in these cells. Full-length TPX2 and TPX2-710 Bac Cells were co-nucleofected with siRNA to deplete endogenous TPX2 and with a plasmid encoding mCherry-Kif15. 40 h after nucleofection, cells were treated with STLC for 18h and spindle morphology distribution was scored. Bipolar spindles were present in the majority of cells expressing full-length

TPX2 but not in cells expressing TPX2-710 (Fig 3.4D). This result demonstrates that the C-terminal region of TPX2 is necessary for Eg5-independent bipolar spindle formation in cells expressing elevated levels of Kif15.

The mechanism by which Kif15 promotes spindle bipolarity in the absence of Eg5 activity is not known but has been proposed to result from Kif15 action on parallel, bundled microtubules (Sturgill and Ohi, 2013). Consistent with this, recent work shows that some kinesin-5 inhibitor–resistant cell lines express low levels of a rigor mutant of Eg5 that promotes microtubule bundle formation (Sturgill et al., 2016). To determine whether microtubule bundles are sufficient for Kif15 localization in the absence of TPX2, endogenous TPX2 was depleted from cells and were then treated with 2-[1-(4-fluorophenyl)cyclopropyl]-4-(pyridin-4-yl)thiazole (FCPT), which induces microtubule bundle formation by promoting rigor binding of Eg5 to microtubules (Groen et al., 2008). Treatment of parental cells with FCPT alone promoted microtubule bundle formation as expected; however, very few bundles were observed in the absence of TPX2 (Fig 3.4E). Immunostaining showed that Eg5 bound to microtubule bundles in FCPT-treated control cells, was reduced in siTPX2-treated cells, and bound to residual bundles in cells treated with both FCPT and siRNA to TPX2 (Fig 3.4E). Although Kif15 was detected on bundles in FCPT-treated control cells, it was not detected in cells treated with siRNA targeting TPX2, even when FCPT was added to promote bundle formation (Fig 3.4E). These results show that Eg5 can bind to spindle microtubules in the absence of TPX2 when rigor binding of Eg5 to microtubules is promoted by FCPT treatment. However, in cells lacking TPX2, the formation of microtubule bundles using FCPT treatment alone may not be sufficient to localize Kif15 properly to the spindle.

3.2.4 Dynamic microtubules contribute to Kif15 behavior in vivo

Although Kif15 motility in vitro has been characterized (Drechsler et al., 2014; Sturgill et al., 2014), the motile behavior of Kif15 in vivo has not been reported. To investigate this, time-lapse confocal microscopy was performed on GFP-Kif15–expressing LLC-Pk1 cells, which remain relatively flattened during mitosis, facilitating imaging. Rapid motion of fluorescent particles of GFP-Kif15 moving toward the spindle equator were observed, where microtubule plus ends are located (Fig 3.5A). Close inspection of the confocal image sequences revealed some variation in the fluorescence intensity and morphology of the motile particles (Fig 3.5A). The larger or brighter particles may represent clusters of Kif15 tetramers, a possibility that is consistent with recent *in vitro* experiments that show accumulation of Kif15 at intersections of dynamic microtubules and at microtubule plus ends (Drechsler and McAinsh, 2016). However, the fluorescent puncta move rapidly and photobleach quickly, so variation in morphology of individual puncta could not be quantified. When cells progressed into anaphase, GFP-Kif15 was enriched along kinetochore fibers and in some cases showed an accumulation near kinetochore fiber plus ends (Fig 3.5B).

TIRF microscopy of live cells was performed to visualize motors on microtubules that extended to the peripheral regions of the cell (Gable et al., 2012). In accord with results from confocal microscopy, GFP-Kif15 motors appeared to move in a directed manner, away from the centrosome, consistent with predominantly plus end–directed motion (Fig 3.5D).

To determine whether the fluorescent particles of GFP-Kif15 were walking along the lattice of spindle microtubules or moving with the tips of growing microtubules, the

velocity of GFP-Kif15 in vivo from kymographs from fluorescent particles were measured in the image sequences taken of metaphase and anaphase cells (Fig 3.5C). Using identical imaging parameters, LLC-Pk1 cells expressing GFP-EB1 was also imaged to determine the rate of microtubule growth (Piehl et al., 2004). This analysis showed that particles of GFP-Kif15 moved in a processive manner at a velocity of 133 ± 43 nm/s. This value was not different from the rate of microtubule growth determined from the GFP-EB1 movies, 119 ± 26 nm/s ($p = 0.09$) suggesting that Kif15 motility results from association with growing microtubule ends. When imaged at room temperature to reduce photobleaching, velocities observed for both GFP-Kif15 and GFP-EB1 were not different (unpublished data). The relatively wide distribution in the velocities of GFP-Kif15 puncta could reflect different rates for single or multiple motors, for motors walking on one microtubule with a second microtubule as cargo, or because some motors are moving on microtubule growing ends and others are walking along the microtubule lattice (Drechsler and McAinsh, 2016). To determine whether this motile behavior is unique to GFP-Kif15, Eg5-Emerald was overexpressed from a plasmid and the cells were then imaged. In this case, plus end–directed motile behavior was not observed (unpublished data), consistent with previous work demonstrating that Eg5, expressed from a BAC, bound and unbound rapidly from mitotic microtubules and showed dynein-dependent minus-end motion (Uteng et al., 2008; Gable et al., 2012).

To determine whether GFP-Kif15 motility results from motors associating with dynamic microtubule plus ends (Drechsler and McAinsh, 2016), GFP-Kif15 cells were treated with nanomolar concentrations of paclitaxel to suppress microtubule dynamics (Yvon et al., 1999). Under these conditions, the velocity and number of growing

microtubule plus ends measured in GFP-EB1–expressing LLC-Pk1 cells was reduced, confirming a suppression of microtubule dynamics (Data not shown). Time-lapse movies of paclitaxel-treated GFP-Kif15 cells showed a dramatic reduction of Kif15 motility on the spindle, which precluded tracking (Fig 3.6A). This result shows that microtubule dynamics contributes to GFP-Kif15 behavior in vivo. Because of the high density of microtubules in the spindle and the fact that the Kif15 antibody is compatible only with methanol-fixed cells, colocalization of Kif15 and GFP-EB1 in fixed cells could not be observed, and in live cells, expression of both GFP-Kif15 and mCherry-EB1 resulted in aberrant spindle morphology.

To determine whether the distribution of Kif15 and TPX2 was altered in paclitaxel-treated cells, as might be expected if the motors preferentially associate with dynamic microtubules, LLC-PK1 parental cells were fixed and stained for microtubules and TPX2 or Kif15. The results show that suppression of dynamics with paclitaxel resulted in an increase in TPX2 and Kif15 near the spindle poles and a reduction along spindle microtubules (Fig 3.6B). To quantify this, TPX2 and Kif15 fluorescence intensity levels was normalized to tubulin and the ratio of each protein in the half-spindle and at the pole was determined. The results show that paclitaxel treatment reduced this ratio for both Kif15 and TPX2 (Fig 3.6C). Thus the distribution of TPX2 and Kif15 is affected by microtubule dynamics, consistent with the enrichment of TPX2 and Kif15 at plus ends of dynamic microtubules observed *in vitro* (Roostalu et al., 2015; Drechsler and McAinsh, 2016; Reid et al., 2016). Kif15 and TPX2 lack a short amino acid motif composed of serine, any amino acid, isoleucine, and proline (SxIP) that is commonly found in proteins that localize to microtubule plus ends in an EB-1–dependent manner (Honnappa et al.,

2009). This suggests that the association of TPX2 and Kif15 with microtubules may be direct rather than mediated by EB1. TPX2 has been reported to associate with dynamic microtubule ends *in vitro* at low concentrations (Roostalu et al., 2015; Reid et al., 2016) but has not been reported to tip track *in vivo*, where it is present at higher concentrations. One possibility is that TPX2 is required to load Kif15 onto microtubules but not for it to remain at the growing plus end (Fig 3.6B); alternatively, TPX2 may remain at the plus end with Kif15 (Fig 3.6B) but not be detectable in vivo (Roostalu et al., 2015; Drechsler and McAinsh, 2016; Reid et al., 2016).

3.3 Discussion

3.3.1 Role of TPX2 C-terminal region in recruiting Kif15 onto the spindle

The experiments in this chapter show that Kif15 requires the C-terminal region of TPX2 for its localization onto the spindle microtubules. Hence, the same region of TPX2 plays an important for regulating two kinesins Eg5 and Kif15 in cells. This effect is also supported by *in vitro* experiments which show that TPX2 is able to regulate these molecules only when the C-terminal region of amino acids is present. Though the motion on microtubules of both motors is inhibited by full length TPX2, there are differences in the level of inhibition achieved by C-terminally truncated TPX2-710. TPX2-710 does not show an inhibitory effect of Kif15 motion on single microtubules but shows inhibitory effect on Eg5. This difference in regulation of Eg5 and Kif15 observed *in vitro* could be attributed to the differences in the structure and biophysical properties of the two motors. Eg5 has been shown to have unique sequences in the neck linker and stalk region which may account for this (Waitzman and Rice, 2011).

The kinase Aurora A phosphorylates Kif15 in the tail region and enhances the localization onto the spindle and thus plays a role in recruiting the motor molecules onto the microtubules in cells. As TPX2 is necessary for activating Aurora A, it is possible that the inability of TPX2-710 to recruit Kif15 onto the spindle could be an indirect consequence of Aurora A inactivity. However, the staining experiments with phospho Aurora A antibody show that there is a pool of active Aurora A found near the spindle poles. This suggests that mode of action TPX2 C-terminus is recruiting Kif15 onto the spindle may be independent of the Aurora A activation by TPX2. One potential way by which TPX2 C-terminus can enhance Kif15 recruitment could be through formation of microtubule bundles as this region has been demonstrated to be necessary to form cold stable K-fibers (Ma et al., 2011) and Kif15 has been shown to be acting predominantly on parallel bundles of microtubules (Sturgill and Ohi, 2013; Sturgill et al., 2014).

3.3.3 How TPX2 effects in Kif15 force generation in Kif15 overexpressing cells

In Kif15-overexpressing cells have been shown to form bipolar spindles in an Eg5 independent manner as evidenced by formation of bipolar cells when they are treated with STLC. In these cells, spindle formation is believed to occur when a monopolar spindle breaks symmetry, driven by Kif15 acting on parallel, bundled microtubules (Sturgill and Ohi, 2013; Sturgill et al., 2014). Results here show that when TPX2 is depleted from these Kif15-overexpressing cells, bipolar spindles are not observed. One possibility is that TPX2 is needed to generate microtubule bundles to which Kif15 binds (Sturgill et al., 2014) and once bound to these microtubule bundles, Kif15 may act to generate outward force required for the break of symmetry. Alternatively, TPX2 may play a more direct role in promoting force generation by Kif15 by modulating the stall

force of the motor on the microtubule (Drechsler et al., 2014). As the experiments in this chapter show that only full length TPX2 has any significant effect on Kif15 motion on microtubules, it is possible that direct role if any of TPX2 in modulating the force generation capacity may be mediated through the C-terminal residues of TPX2.

3.3.3 Behavior of Kif15 on spindle microtubules in vivo

The results in this chapter show that GFP-Kif15 particles demonstrated plus-end directed motion in different stages of cell cycle. In live cells, Kif15 puncta moved at a rate (133 nm/s) that was indistinguishable from microtubule plus-end growth in LLC-PK1 cells (119 nm/s) suggesting that the some Kif15 puncta may be plus-end tip tracking. This is supported by the observation that treatment with paclitaxel to reduce microtubule dynamics also reduced the plus-end directed streaming motion of Kif15 punctae. Thus, these observations support the idea that motion of Kif15 is due, at least in part, to tracking with microtubule plus ends. This interpretation is also consistent with previous *in vitro* experiments which show that Kif15 tracks, and accumulates at, the plus ends of dynamic microtubules, independent of any other microtubule-associated proteins (Drechsler and McAinsh, 2016). The velocity of GFP-Kif15 puncta in live cells overlaps with the velocity of GFP-Kif15 from cell extracts measured *in vitro* on stable microtubules (~130 nm/s). The similarity of the velocities of microtubule growth and Kif15 puncta motility is these cells is thus consistent with motors tracking plus ends, but the possibility that Kif15 particles are also walking on spindle microtubules *in vivo* cannot be eliminated. Because puncta composed of multiple tetramers of GFP-Kif15 are easier to detect in live cells, our imaging experiments may preferentially capture the

brighter puncta at microtubule ends, and individual motors on the microtubule lattice may be insufficiently bright to track.

If Kif15 molecules tip tracks the plus-ends of growing microtubules in addition to its walking on the spindle microtubules, the functional relevance of this behavior is a very interesting question. One possible explanation is that Kif15 can walk along a kinetochore microtubule while being associated with the growing end of a dynamic microtubule. Such an action of Kif15 would result in aligning of microtubules as bundles in the half spindle. This is especially relevant because in cells as nascent microtubules can be formed from existing microtubules through branching (Petry et al., 2015) and this mode of action of Kif15 can help in aligning them to form microtubule bundles which may contribute to increased k-fiber stability.

3.4 Methods

3.4.1 Materials

All chemicals, unless otherwise specified, were purchased from Sigma-Aldrich.

3.4.2 Cell culture, nucleofection, and inhibitor treatments

LLC-Pk1 cells were cultured in a 1:1 mixture of F10 Ham's and Opti-MEM containing 7.5% fetal bovine serum and antibiotics and maintained at 37°C and 5% CO_2. LLC-Pk1 cells were nucleofected using an Amaxa Nucleofector (Lonza, Basel, Switzerland) using program X-001 and Mirus nucleofection reagent (Mirus Bio, Madison, WI) according to the manufacturers' recommendations. The following siRNAs were used: TPX2, GGACAAAACUCCUCUGAGA; Nuf2, AAGCAUGCCGUG-

AAACGUAUA; and Kif15, UGACAUCACUUGCAAAUAC. siRNAs were purchased from Dharmacon (GE Healthcare Life Sciences, Pittsburgh, PA).

LLC-Pk1 cells expressing full-length TPX2 or TPX2-710 from a BAC were grown as previously described (Ma et al., 2011). To generate cells expressing GFP-Kif15, parental cells were nucleofected with GFP-Kif15 and selected using the appropriate antibiotic; cells were subcloned to enrich for GFP-Kif15–expressing cells. For some experiments, GFP-Kif15 cells that had been further selected for fluorescence using cell sorting were used. mCherry-Kif15 was prepared by subcloning of GFP-Kif15 into the appropriate vector.

Paclitaxel, FCPT, and STLC were prepared as stock solutions in dimethyl sulfoxide, stored at –20°C, and diluted with culture medium before use. FCPT was used at 200 μM, paclitaxel at 330 nM, and STLC at 1 μM.

3.4.3 Preparation of cell extracts

Cell extracts for TIRF experiments were prepared from LLC-Pk1 cells expressing GFP-Kif15. A confluent 100-mm-diameter cell culture dish was washed twice with calcium and magnesium-free phosphate-buffered saline (PBS), and then 300 μl of extraction buffer (40 mM 4-(2-hydroxyethyl)-1-piperazineethanesulfonic acid/KOH, pH 7.6, 100 mM NaCl, 1 mM EDTA, 1 mM phenylmethylsulfonyl fluoride, 10 μg/ml leupeptin, 1 mg/ml pepstatin, 0.5% Triton X-100, and 1 mM ATP) was added dropwise to the dish and incubated with gentle rotation for ~2 min (Cai et al., 2007; Balchand et al., 2015). The extract was transferred to a microcentrifuge tube on ice and centrifuged at 15,000 rpm at 4°C for 10 min in a tabletop centrifuge. The supernatant

was recovered and used immediately or stored in aliquots in liquid nitrogen; protein concentration was determined using the method of Lowry et al. (1951). For quantification of the fluorescence intensity of individual puncta using TIRF microscopy, the cells were treated with siRNA targeting endogenous Kif15 72 h before preparation of the extract.

To prepare mitotic extracts, GFP-Kif15 cells were treated with siRNA targeting endogenous Kif15 and synchronized using 330 nM nocodazole for the final 18 h of the 72-h siRNA treatment. Extracts were prepared as described, with the addition of Simple Stop 1 Phosphatase Inhibitor Cocktail (1X; Gold Biotechnology, St. Louis, MO) to the extract buffer.

3.4.4 Protein purification

Full-length and truncated TPX2 were expressed and purified from bacteria as previously described (Balchand et al., 2015). Kinesin-1–GFP was prepared using the dimeric construct as previously described (Balchand et al., 2015). To generate TPX2-657, a stop codon was introduced at amino acid 657 in the bacterially expressed full-length TPX2 construct. To generate TPX2-ΔPFAM, PCR was used to remove amino acids 662–719 from full-length TPX2. Proteins were run on 8% polyacrylamide gels using appropriate molecular weight standards and stained with Coomassie brilliant blue.

3.4.5 Single-molecule experiments

The single molecule experiments were performed as described in chapter 2. Briefly, perfusion chambers (~10-µl volume) were made from glass slides, silanized coverslips, and double-stick tape (Balchand et al., 2015). 10 µl of 10% rat YL ½ anti-

tubulin antibody followed by 5% Pluronic F-127 and the by Diluted rhodamine-labeled microtubules composed of 10% rhodamine tubulin were flowed into the chamber with 3 min incubations. Following a second block of 5% Pluronic F-127 for 3 min, cell extract containing GFP-Kif15 diluted in PEM 20 motility buffer (20 mM 1,4-piperazinediethanesulfonic acid, pH 6.9, 2 mM ethylene glycol tetraacetic acid, 2 mM $MgSO_4$) containing 0.25% F127, 100 μM ATP, 1 mM dithiothreitol, and 25 μM paclitaxel and supplemented with an oxygen-scavenging system (15 mg/ml glucose, 1.23 mg/ml glucose oxidase, and 0.375 mg/ml catalase) was flowed into the chamber, and imaged. To determine the directionality of Kif15, polarity-marked microtubules were used, and it was confirmed that Kif15 walked toward the plus end for the majority of excursions. For preincubation experiments with TPX2, the indicated concentrations of TPX2 were added to the motility buffer containing GFP-Kif15 and incubated on ice for 2 min before flowing into the chamber. Single-molecule imaging of kinesin-1–GFP was performed as described previously (Balchand et al., 2015).

3.4.6 Microscope imaging and analysis

TIRF microscopy was performed using a Nikon (Melville, NY) Ti-E microscope with a 100×/1.49 numerical aperture (NA) objective lens and an Andor (Belfast, UK) Zyla scientific complementary metal-oxide semiconductor camera; the system was run by Nikon Elements software. TIRF imaging was performed at room temperature; images were collected at 1 frame/s for a total of 300 s. To measure motor velocity, individual puncta were tracked using the Particle Tracking function of Nikon Elements software and exported to Excel for analysis. For the experiment with mitotic extract, a Nikon Ti-E

microscope run by MetaMorph software and with a Hamamatsu Flash 4.0 camera was used.

Live and fixed cells were imaged using either spinning-disk confocal microscopy or point-scanning confocal microscopy. For spinning-disk confocal microscopy, two different systems were used, either a Nikon Ti-E microscope with a CSU-X1 Yokogawa spinning-disk confocal scan head (PerkinElmer, Wellesley, MA), an Andor iXon+ electron-multiplying charge-coupled device camera (Andor), and a 100×/1.4 NA objective lens or a CSU-10 Yokogawa spinning-disk confocal microscope on a Nikon TE300 as previously described (Tulu et al., 2003). For live-cell imaging, exposures were adjusted without saturating the camera's pixels; typical exposures were 50–800 ms. For point-scanning confocal microscopy, a Nikon A1R system with a 60×/1.4 NA objective lens was used. Images of live cells were acquired every 2 s at room temperature or every 3 s at ∼34°C; images were typically collected for 2–5 min. For both fixed- and live-cell imaging, a laser power of 1–2% was used. For heating the cells during imaging, a Nicholson Precision Instruments (Bethesda, MD) Air Stream Stage Incubator was used; temperature was measured using a thermistor probe taped to the microscope stage outside of the cell chamber. When the thermistor temperature is 37°C, the temperature inside the chamber is ∼34°C.

To quantify the fluorescence intensity of tubulin and Kif15, a 1 × 1 μm box was placed midway between the spindle pole and the chromosomes or at the spindle pole, and the ratio of Kif15 to tubulin fluorescence was measured after background subtraction. Statistical analysis was performed in Excel. Velocity of GFP-EB1 dashes and Kif15 puncta were tracked in ImageJ using the M Track J plug-in.

3.4.7 Immunofluorescence

LLC-Pk1 cells were plated on #1.5 glass coverslips ~48 h before experiments. For Kif15 staining, cells were rinsed twice with room temperature PBS lacking calcium and magnesium, fixed in −20°C methanol for 5–10 min, and rehydrated in PBS containing 0.1% Tween and 0.02% sodium azide (PBS-Tw-Az). Kif15 primary antibodies (Cytoskeleton, Denver, CO) were used following the manufacturer's recommendation and subsequently stained with fluorescent secondary anti-rabbit antibodies (Ma et al., 2011). For TPX2 staining, cells were fixed in 2% paraformaldehyde, 0.25% glutaraldehyde, and 0.5% Triton X-100 made fresh daily in PBS lacking calcium and magnesium. TPX2 antibodies were obtained from Novus Biologicals (Littleton, CO); Hec1 antibodies (Abcam, Cambridge, MA) were the kind gift of T. Maresca (University of Massachusetts). Microtubules were stained with either DM1a mouse anti-tubulin (Sigma Chemical Co.) or YL1/2 rat anti-tubulin (Accurate Chemical and Scientific, Westbury, NY) and appropriate secondary antibodies as previously described (Ma et al., 2011). Stained cells were mounted on glass slides using Fluomount G (Southern Biotech, Birmingham, AL) to which 4′,6-diamidino-2-phenylindole was added to stain DNA.

3.4.8 Western blotting and detection

Whole-cell extracts of control or siRNA-treated cells were prepared by adding SDS sample buffer to 35-mm dishes of cells, followed by sonication. Extracts were run on 8% SDS polyacrylamide gels using the formulation of Laemmli (1970). Gels were transferred onto Amersham Hybond-P membrane (GE Healthcare, Waukesha, WI). Blots

were probed with Kif15 or TPX2 antibodies used at 1:1000 for 1 h at room temperature in 5% nonfat dry milk dissolved in Tris-buffered saline containing 0.02% Tween-20 (TBS-Tween). The blots were then probed with goat anti-rabbit horseradish peroxidase–conjugated secondary antibody (1:5000; Jackson ImmunoResearch Laboratories, West Grove, PA) for 1 h at room temperature in 5% nonfat dry milk dissolved in TBS-Tween and detected using chemiluminescence.

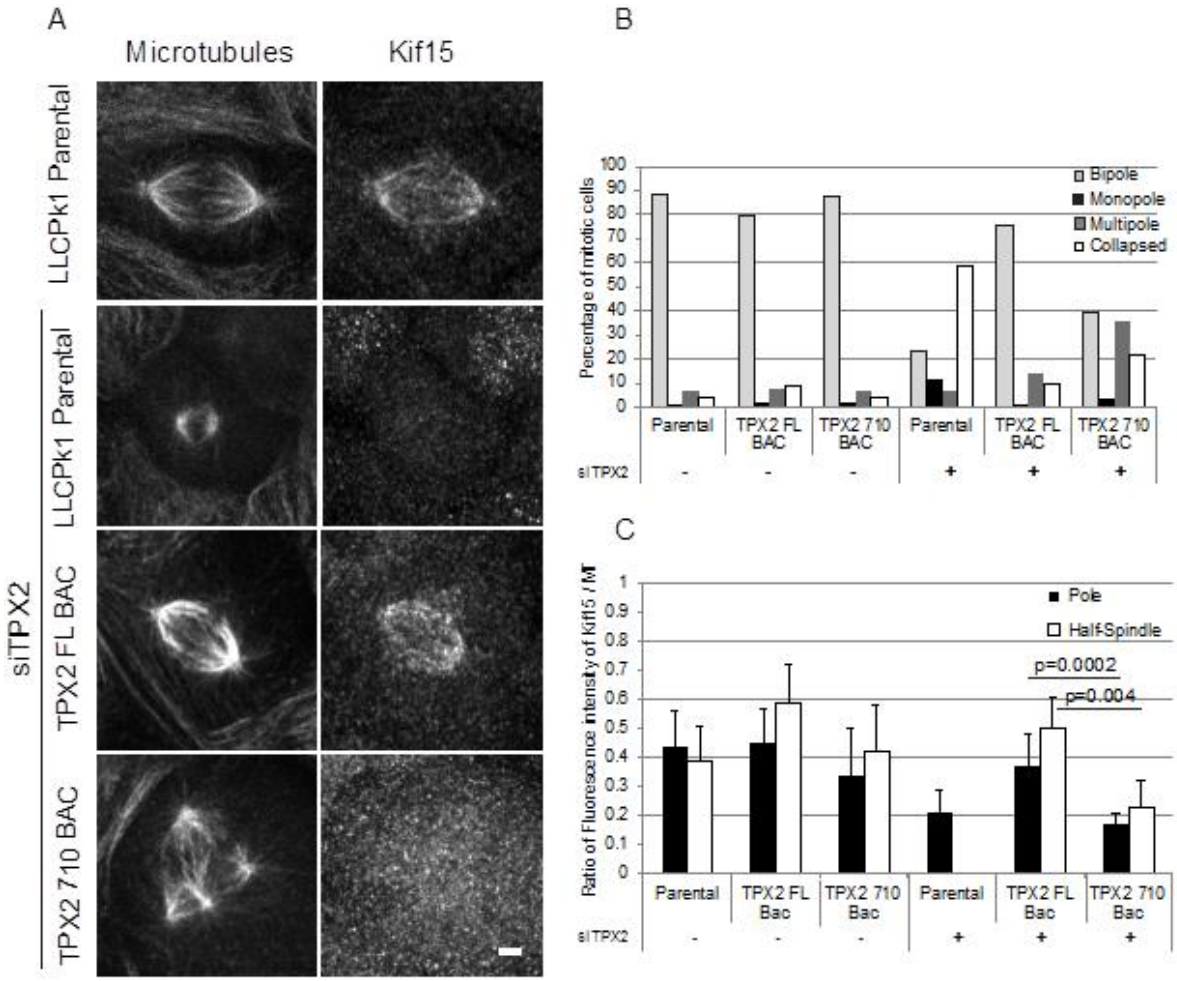

Figure 3.1 The C-terminal region of TPX2 contributes to spindle localization of Kif15. (A) Immunofluorescence staining for microtubules (left) and Kif15 (right). Top, parental cells; the remaining three rows show cells depleted of TPX2 and expressing no transgene (parental), transgene encoding full-length TPX2 (middle), or TPX2-710 (bottom). Scale bar, 2 μm. (B) Spindle morphology for parental cells and cells expressing full-length or truncated TPX2; cells on the right were additionally treated with siRNA targeting TPX2. (C) Quantification of fluorescence ratio of Kif15 to tubulin at pole and in the half-spindle. Error bars are SD. Parental cells depleted of TPX2 were only measured at spindle pole due to loss of spindle microtubules.

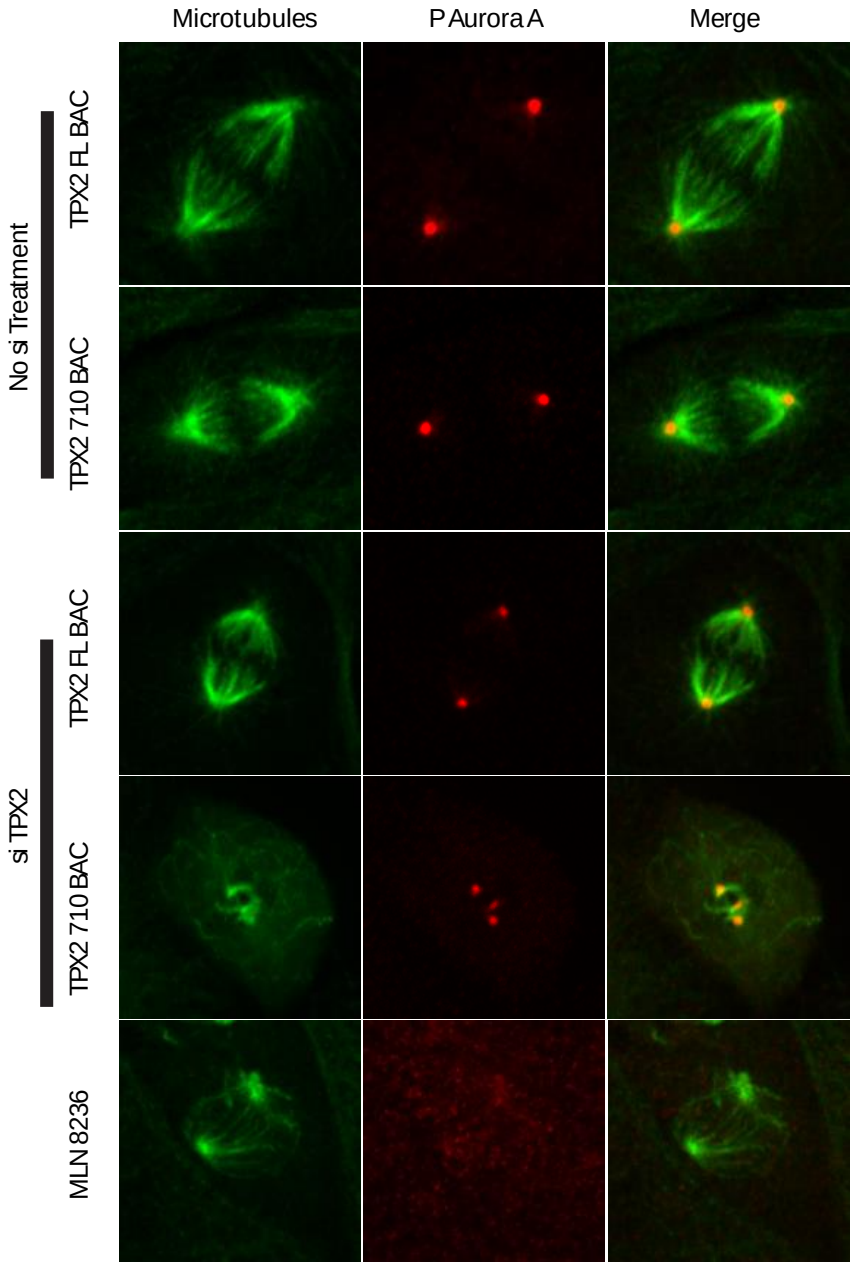

Figure 3.2 Removal of TPX2 C terminus does not abolish Aurora A kinase activity. Immunofluorescence staining of microtubules and p Aurora A of control or siTPX2 treated LLCPK1 cells expressing TPX2 FL or TPX2 710 bacterial artificial chromosome transgene. The bottom panel shows the staining in LLCPK1 parental cells treated with Aurora A inhibitor MLN8236.

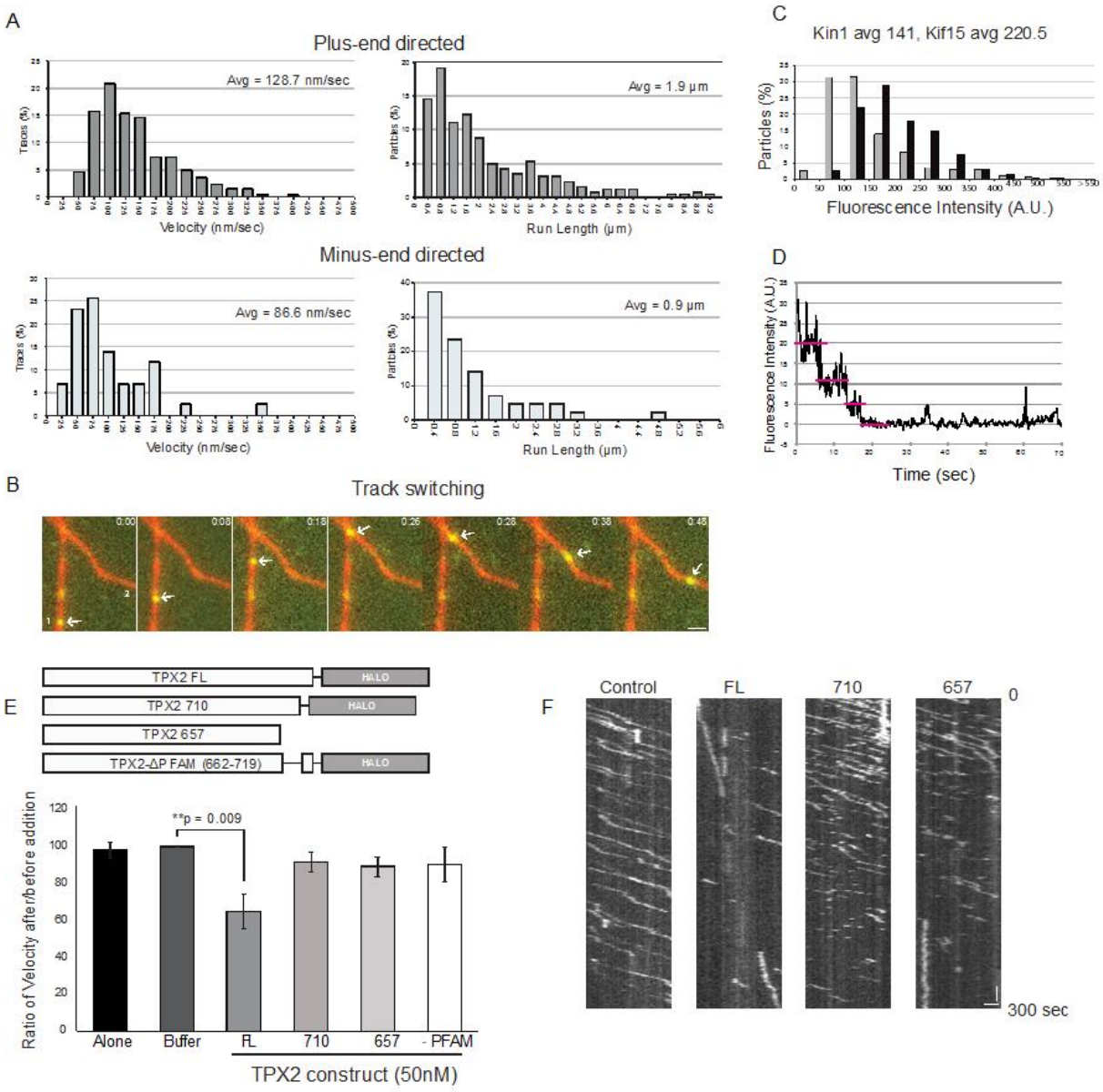

Figure 3.3 Inhibition of Kif15 motor stepping requires full-length TPX2. (A) Histograms of GFP-Kif15 velocity (left) and run length (right) for plus end– and minus end–directed motion; *n* = 261 and 43 motors, respectively. Data from two independent experiments. (B) GFP-Kif15 switches microtubule tracks; arrow marks moving GFP-Kif15 puncta. Time in minutes:seconds. Bar, 1 µm. (C) Histogram of fluorescence intensity of kinesin-1–GFP (top) and GFP-Kif15 (bottom); fluorescence in arbitrary units (A.U.). For kinesin-1–GFP, *n* = 295, and for GFP-Kif15, *n* = 652, from two independent

experiments. (D) Photobleaching of microtubule-bound GFP-Kif15 from interphase and mitotic extracts. Horizontal pink lines show bleach steps. For interphase, n = 11 particles, five with more than three steps and six with fewer than three steps; data from two independent experiments; for mitotic extracts, n =15 particles, 10 with more than three steps and five with fewer than three steps. (E) Schematic diagram of constructs used for inhibition experiments (top) and bar graph (bottom) showing ratio of velocity without and with added proteins; error bars, SEM. (F) Kymographs showing motility of GFP-Kif15; added TPX2 construct indicated at the top; vertical axis marker bar, 15 s; horizontal axis marker bar, 1 μm.

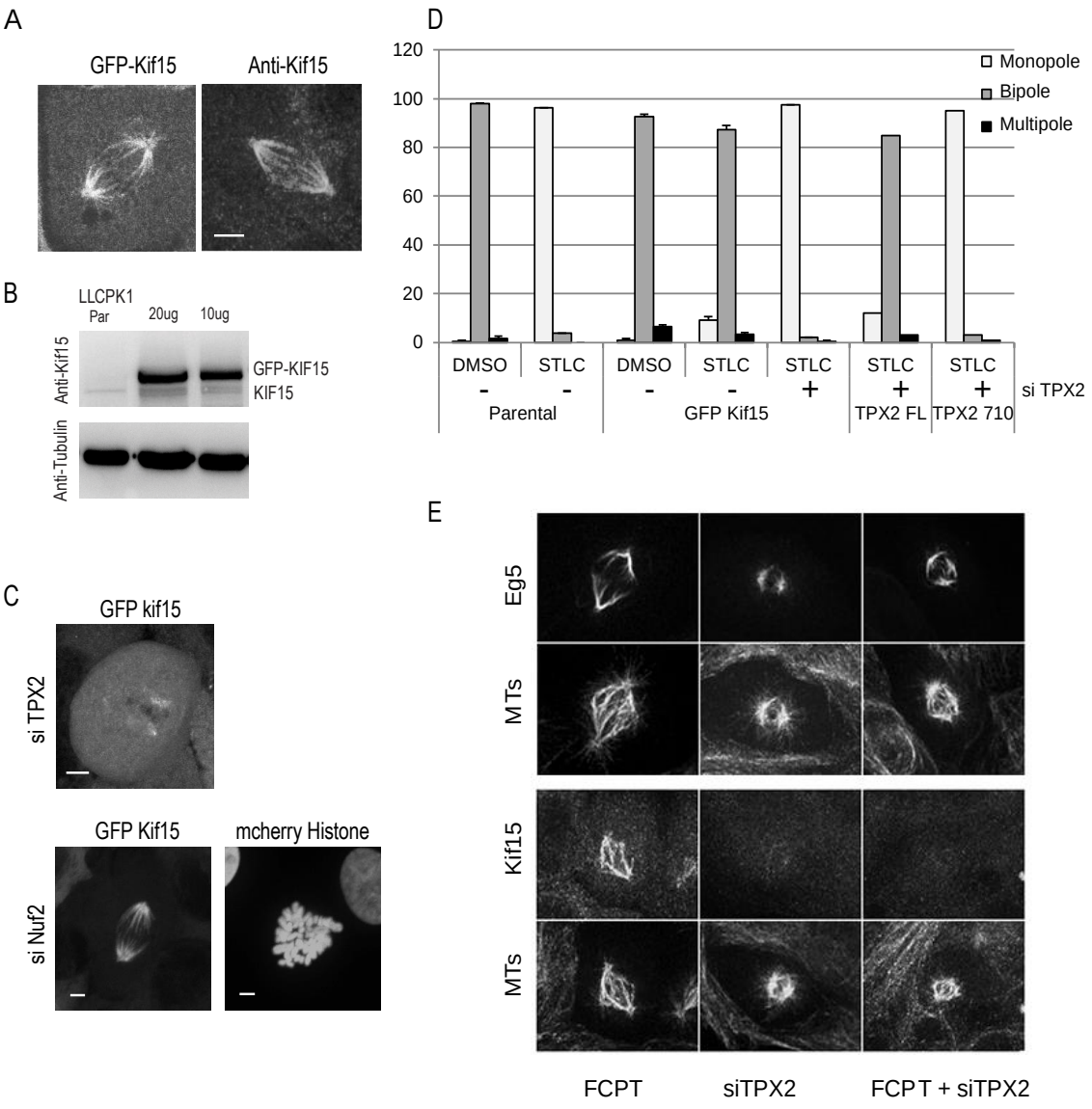

Figure 3.4 TPX2 is required for bipolar spindle formation in cells overexpressing Kif15. (A) LLC-Pk1 cells expressing GFP-Kif15 (left) and parental cells fixed and stained for Kif15 (right). (B) Western blot of extracts from parental and GFP-Kif15–expressing cells; blot stained for Kif15 (top) and tubulin as loading control (bottom). (C) Images of GFP-Kif15–expressing cells treated with siRNA targeting TPX2 (top) or Nuf2 (bottom); GFP-Kif15 (left) and co-nucleofected mCherry-H2B to label chromosomes (right). (D) Bar graphs showing percentage of bipolar, monopolar, and multipolar spindles for each treatment condition. Error bars show SD. (E) Parental cells treated with FCPT, with siRNA targeting TPX2, or with both. Cells were stained for microtubules (bottom) and either Kif15 or Eg5 (top). Bar, 2 μm.

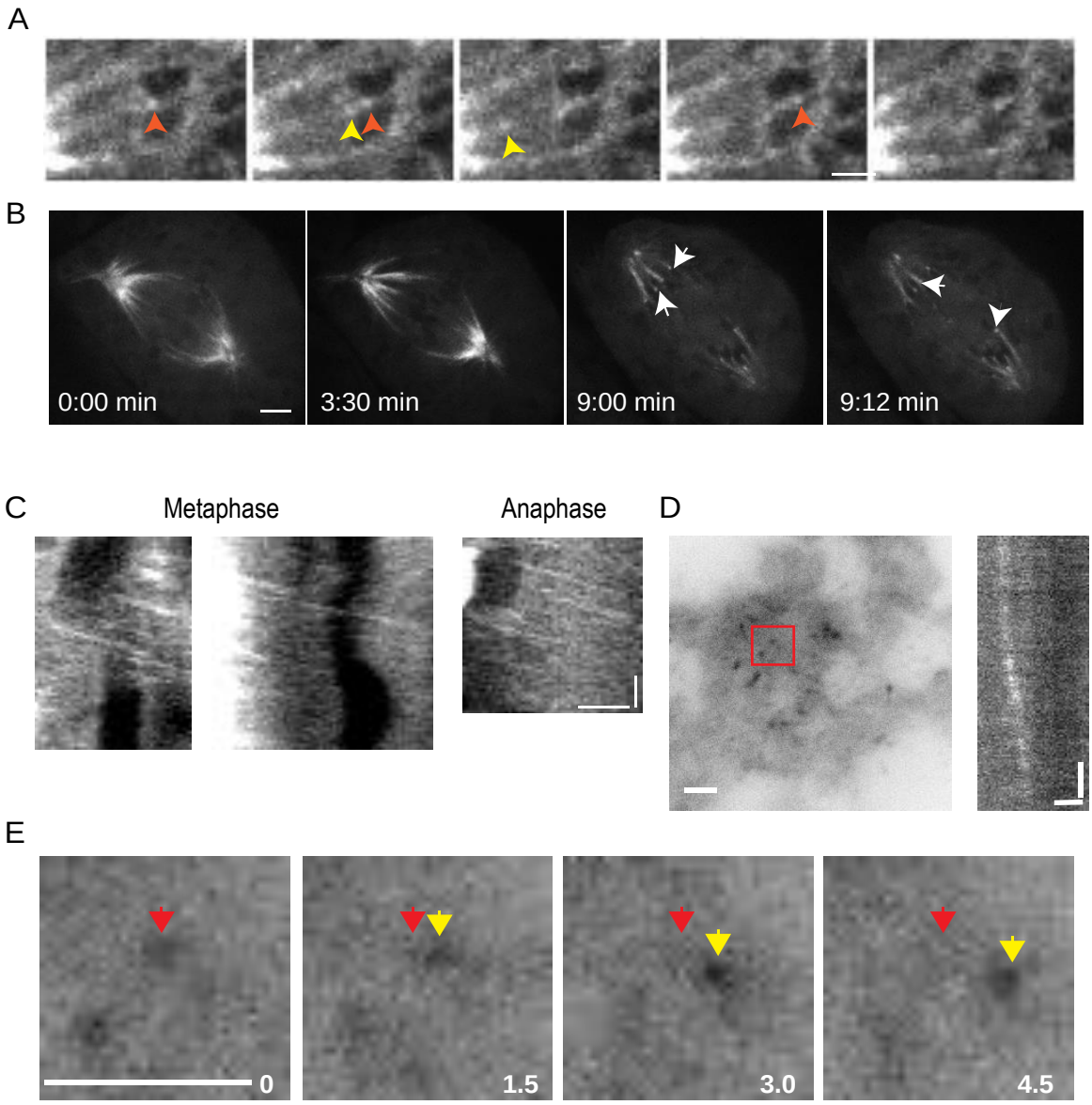

Figure 3.5 Dynamics of GFP-Kif15 *in vivo*. (A) Selected frames from a movie of GFP-Kif15 expressing cells; red and yellow arrowheads mark fluorescent particles traveling toward the chromosome region (spindle equator to the right; dark ovals are chromosomes). (B) Live cell expressing GFP-Kif15 progressing from prometaphase (0:00) to metaphase (3:30) and anaphase (9:00); arrows show accumulation of fluorescence near the kinetochores. (C) Kymographs from movie sequences of GFP-Kif15–expressing metaphase and anaphase cells; dark regions are chromosomes; spindle midzone to right. (D) TIRF microscopy of GFP-Kif15 expressing cells; Kymograph of an individual puncta of GFP-Kif15 (right panel). (E) Region marked with red box in (D) is shown enlarged in panels; red arrowhead shows initial position of puncta (contrast inverted); yellow arrow marks puncta. Time in sec. Time: vertical axis; distance: horizontal axis. Scale: Horizontal bar 2 μm. Vertical Bar 30s in (C) and 2s in (D).

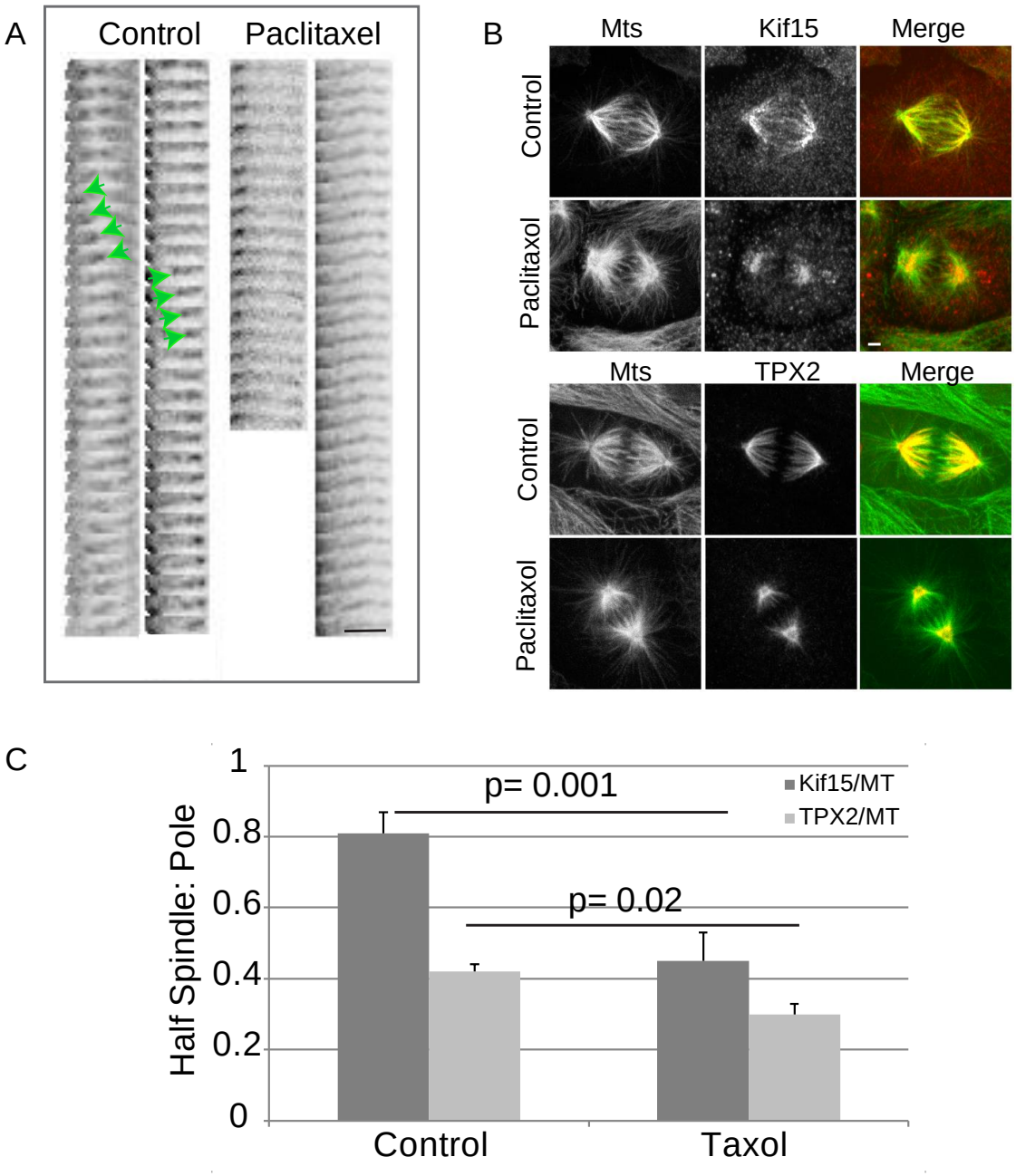

Figure 3.6 Microtubule dynamics contribute to spindle distribution of Kif15. (A) Sequential frames (2-s interval) from movies of GFP-Kif15 expressing control and paclitaxel-treated cells (inverted contrast); motion of fluorescent particles toward the kinetochore region (right) in control but not paclitaxel-treated cells. Green arrowheads mark moving puncta. (B) LLC-Pk1parental cells fixed and stained for microtubules and Kif15 (top) or TPX2 (bottom); control and paclitaxel as indicated; merged images to the right. (C) Bar graph showing ratio of fluorescence intensities of Kif15 and TPX2 to microtubules of images shown in (B). Scale Bar, 2 μm.

CHAPTER 4

GENERAL DISCUSSION

4.1 Chapter summaries

Eg5 and Kif15 are the two major motor proteins that generate plus-end directed forces on the spindle and are necessary for generation and maintenance of spindle bipolarity. Both Eg5 and Kif15 have been previously demonstrated to be regulated by the microtubule associated protein TPX2. How TPX2 molecules interact with the motors Eg5 and Kif15 on the microtubules is incompletely understood. Through a combination of *in vitro* reconstitution TIRF experiments and live cell imaging, the results presented in these chapters help in understanding the mechanism and requirements for the regulation of both Eg5 and Kif15 by TPX2.

In chapter 2, the microtubule co-sedimentation experiments showed that TPX2 binds tightly to microtubules with nanomolar affinity and that the C-terminal residues of TPX2 do not play a significant role in the microtubule binding in bulk sedimentation assays. This binding interaction was found to be electrostatic but independent of the charged C-terminal E-hook region of tubulin. Characterization of Eg5-EGFP from cell extracts showed that cell extracts can be an excellent source of highly functional Eg5 motor proteins with very similar biophysical properties compared to Eg5 molecules purified from Sf9 insect cells. *In vitro* TIRF experiments showed that full length TPX2 is a more potent inhibitor of Eg5 motion on single microtubules than the C-terminally truncated TPX2-710, which also inhibits Eg5 motion albeit to a lesser extent. This

differential inhibition by TPX2 molecules was also observed in microtubule surface gliding experiments with Eg5 dimers but not Eg5 monomers.

The results from these experiments suggest a model where both full length TPX2 and TPX2-710 can bind to microtubules and inhibit Eg5 motion on microtubules by acting as a road block. The more potent inhibition of Eg5 achieved by full length TPX2 which contains the Eg5 interaction domain suggests that the C-terminal amino acids of TPX2 may act as tether or brake on Eg5 molecules resulting in the stronger inhibition. The microtubule surface gliding experiments, using dimeric and monomeric constructs of the motor, suggest that the amino acid residues present in the stalk and neck-linker region of Eg5 are involved in Eg5-TPX2 regulation. These residues on Eg5 could be directly involved in Eg5-TPX2 interaction. Alternately, they may be involved in the formation of a specific Eg5 conformation that TPX2 recognizes resulting in the inhibition of Eg5 motion on microtubules. The results from these experiments help characterize how TPX2 regulates Eg5 by acting as a brake and a tether at the molecular level.

In chapter 3, results show that the C-terminal region of TPX2 that regulates Eg5 also regulates Kif15 localization to the spindle. Consistently, only full length TPX2 and not truncated constructs of TPX2 were able to regulate motion of Kif15 molecules in *in vitro* TIRF experiments. Aurora A kinase activity was not compromised in the presence of TPX2-710 suggesting that TPX2 mediated regulation of Kif15 may involve a more direct role for TPX2 in localizing Kif15 molecules onto the spindle. Elevated expression of Kif15 has been shown to induce parallel microtubule bundle formation even under the absence of proper microtubule attachments at kinetochore. This chapter shows that even under elevated levels of expression, Kif15 requires TPX2 to localize to microtubules.

When TPX2 is depleted in parental cells, artificial bundling of microtubules in the spindle using FCPT treatment recruits only Eg5 to the spindle but not Kif15. This suggests that within cells, microtubule bundling alone may not be sufficient to recruit Ki15 onto the microtubules. Observation of the dynamics of Kif15-GFP particles in cells revealed plus-end directed streaming motion of the Kif15 particles, which was affected by dampened microtubule dynamics following treatment with paclitaxel. This suggests that some population of the motor may be associated with the growing plus-ends of microtubules and contribute to the observed plus-end streaming motion of Kif15 particles. Thus, the results from this chapter show that TPX2 C-terminus and microtubule dynamics play a role in regulating Kif15 localization and behavior on the spindle.

4.2 Discussion

4.2.1 Microtubule binding of TPX2

The experiments in these chapters show that full length TPX2 binds tightly to microtubules with affinities comparable to some of the other microtubule associated proteins like XMAP215(2μM), She1(.77μM), SKAP(2μM) (Spittle et al., 2000; Markus et al., 2012; Schmidt et al., 2010). Results show that removal of Eg5 interaction domain in TPX2 does not have a large effect on the microtubule binding ability of TPX2. However, removal of Eg5 interaction domain causes significant changes in microtubule organization in mammalian cells and in *Xenopus* extract. Truncation of Eg5 interacting domain in TPX2 abolishes microtubule nucleation from pre-existing microtubules in *Xenopus* extracts (Alfaro-Aco et al., 2017). In mammalian cells, loss of this domain in TPX2 causes loss of cold stable K-fiber formation but does not compromise chromosome

dependent nucleation of microtubules (Ma et al., 2011). Thus, in mammalian cells, the removal of Eg5 interaction domain in TPX2 affects stability of K-fibers but not the nucleation of microtubules around chromosomes. It is not completely clear why the removal of Eg5 interaction domain in TPX2 affects microtubule nucleation only in *Xenopus* extracts but not in cells. It is possible that the last 37 amino acids of TPX2 is essential for microtubule nucleation only in the context of nucleation from pre-existing microtubules but is dispensable for nucleation of microtubules directly from tubulin solutions. Consistent with this, Alfaro-Aco et al., showed that there are constructs of TPX2 lacking the C-terminal region of TPX2 that are capable of binding and nucleating microtubules *in vitro* from tubulin solutions but not form branched microtubules from pre-existing microtubules. These observations suggest that the C-terminal region of TPX2 is involved in nucleation of branched microtubules. TPX2 may also play a role in formation of microtubule bundles by directly binding two or more microtubules through its different microtubule binding domains (Alfaro-Aco et al., 2017) or by recruiting crosslinking motor proteins like Eg5 and Kif15 to these bundles. TPX2 binds to microtubules independent of the charged E-hook region in tubulin, which is required for microtubule binding by most kinesins. As TPX2 binding to microtubules did not prevent microtubule binding of kinesins Eg5, Kif15 or kinesin-1, TPX2 may not occupy the same binding region on microtubules as the kinesins. As most kinesin heads bind along the outer ridge of the microtubule with the binding interface situated in a groove between α and β tubulin heterodimer (Kikkawa et al., 2000), TPX2 may bind to an interface located between the protofilament. I also speculate that the binding of TPX2 on the microtubules could be specifically on the left side of the protofilaments as TPX2 binding to

microtubules does not involve the E-hook which is located on the right side of the protofilaments (Nogales et al., 1998; Kikkawa et al., 2000; Nogales et al., 2016). This may allow TPX2 to regulate kinesins Eg5 and Kif15 without affecting its role in microtubule binding and organization.

4.2.2 Similarities and differences between Eg5 and Kif15

In vitro TIRF experiments discussed in these chapters demonstrate that Eg5 and Kif15 molecules obtained from cell extracts exhibited some similarities and differences in their biophysical properties. Both, Eg5 and Kif15 molecules walked processively towards microtubule plus-ends predominantly and accumulated at plus-end tips of microtubules. Both motors obtained from native cell extracts were mostly tetrameric suggesting that the physiologically relevant oligomeric state for both Eg5 and Kif15 is a tetramer. Eg5 was very slow (14nm/s) when compared with Kif15 (120nm/s) consistent with previous studies (Kwok et al., 2006; Dreschsler et al., 2014). Short minus-end directed runs and microtubule track switching were observed only for Kif15 molecules but not Eg5 which could have some functional consequences. Eg5 molecules are thought to be active mainly on anti-parallel microtubules and Kif15 to be active on parallel microtubules in the spindle (Sturgill et al., 2012). Plus-tip tracking behavior was observed *in vivo* only for Kif15 but not Eg5. Recently, plus end tip tracking was observed for Kif15 molecules *in vitro* and was reported to contribute to sorting and aligning microtubules into parallel bundles (Drechsler et al., 2016). To my knowledge, the results presented here are the first observations of plus-end tip tracking of Kif15 particles within cells which lends support to the *in vitro* study by Drechsler et al., 2016.

4.2.3 How does TPX2 regulate both Eg5 and Kif15 activity in cells

Both Eg5 and Kif15 bind to microtubule pairs and slide them to generate force (Kapitein et al., 2005; Drechsler et al., 2016). However, the orientation of the microtubule pairs required for activity in *in vitro* studies is different for both motors as Eg5 preferentially binds to anti-parallel microtubules and Kif15 preferentially binds to parallel microtubules (van den Wildenberg et al., 2008; Kapitein et al., 2005; Drechsler et al., 2016). When Eg5 binds to anti-parallel microtubules, the motor is switches from a diffusive to directional state and the motor head pairs become engaged on both microtubules resulting in microtubule sliding (Kapitein et al., 2008; Kapitein et al., 2005). The Eg5 motor heads move simultaneously on both microtubules at roughly the same rate and thus the Eg5 dependent microtubule sliding involves coordinated movements of all active motor heads on both microtubules (Kapitein et al., 2005). Eg5 molecules when bound to parallel bundles do not show any microtubule sliding activity and exhibit overlap length dependent resistance to microtubule sliding (Shimamoto et al., 2015). Hence, in this parallel geometry, Eg5 when slowed by TPX2 may just serve to crosslink the microtubules and consequently stabilize parallel microtubule bundles and help form cold stable K fiber.

Unlike Eg5, Kif15 preferentially binds to parallel microtubule pairs. Though Kif15 actively walks on both microtubules, a velocity differential exists between the motor head pairs engaged on the two microtubules (Drechsler et al., 2016). And this velocity differential is necessary for sliding microtubules and generating force specifically when microtubule pairs are in parallel orientation (Drechsler et al., 2016). Thus, for Kif15 dependent sliding of parallel microtubules, one pair of motor heads

walking on the microtubule should be walking slower and for Eg5 dependent anti-parallel microtubule sliding, all motor heads need to engage at roughly the same velocity.

In the context of the cell, Eg5 dependent microtubule sliding is essential for separating the centrosomes and establishing bipolarity early in the cell division but this activity is not essential for maintenance of bipolarity once it is established. Thus, Eg5 activity should be maximal during early stages of cell division and negatively regulated once bipolarity is established. Within cells, Kif15 activity is dispensable for establishment of bipolarity under normal conditions but is required for maintenance of bipolarity after initial establishment. So, Kif15 molecules must stay active during later stages of cell division for maintenance of bipolarity.

Data presented in Chapters 2 and 3 show that TPX2 inhibits motility of Eg5 and Kif15 molecules on single microtubules *in vitro*. However, the inhibitory effect of TPX2 on Eg5 is stronger than its effect on Kif15. This could potentially explain subtle differences in regulation of Eg5 and Kif15 activity within cells. I hypothesize that in cells, TPX2 being a weak inhibitor of Kif15 motion on microtubules, could potentially slow down but not completely stop the Kif15 motor heads on microtubules and create the velocity differential that would aid in Kif15 dependent bundling and sliding of parallel microtubules. Thus, Kif15 regulation by TPX2 may help rearrangement of dynamic microtubules on the spindle into parallel bundles and help stabilize K fibers and maintain bipolarity. By being a stronger inhibitor of Eg5, it could prevent defective spindles from being formed when Eg5 activity is excessive and unregulated (Ma et al., 2011). I also speculate that by strong inhibition of Eg5, TPX2 may force an Eg5 conformation that

helps crosslink parallel bundles during later stages of cell cycle and aid in stabilization of K-fiber.

4.2.4 Future directions

Previous studies have shown that Eg5 and Kif15 possess a second microtubule binding domain in located in their tail region which helps the molecules bundle microtubules with a specific preference to parallel or anti parallel orientation even in the absence of the motor domains (van-Den Wildenberg et al., 2008; Weinger et al., 2011; Sturgill et al., 2014). As regulation of Eg5 and Kif15 by TPX2 have been shown to involve regions other than the motor head, it will be of interest to find the effect of TPX2 on the second microtubule binding domains located in the tail region of both Eg5 and Kif15. The geometry of microtubule orientation is very critical for both Eg5 and Kif15 to elicit proper physiological function and future studies aimed at understanding the effect of TPX2 on Eg5 and Kif15 engaged on microtubule bundles with specific geometries could offer useful insights. Recently Kif15 was shown to be regulated by another MAP called Kinesin Binding Protein (KBP). Interestingly, KBP regulated localization of Kif15 in the equatorial region of the spindle around the chromosomes by interacting directly with the kinesin motor head (Brouwers et al., 2017). TPX2 dependent regulation of Kif15 does not show such specific regional preference and involves the leucine zipper region in the tail region of Kif15 (Tannenbaum et al., 2009). Future *in vitro* studies to determine whether KBP alters motility of Kif15 alone or in conjunction with TPX2 will be of interest. Both Kif15 and TPX2 have been shown to track growing plus-ends of microtubules in *in vitro* experiments (Drechsler et al., 2016; Reid et al., 2016; Roostalu et

al., 2015). It remains to be tested whether TPX2 also plays a role in regulating Kif15 at the microtubule plus-ends thereby potentially altering microtubule dynamics.

4.3 Proposed Model

Based on the results presented here and previously published work, I propose the following model (Fig 4.1). In the presence of full length TPX2 (Left panels), microtubules are nucleated around chromosomes. Presence of full length TPX2 also enhances Eg5 and Kif15 localization onto the spindle microtubules. In the presence of full length TPX2, Kif15 molecules align microtubules into parallel orientation and helps stabilize K fibers. Strong inhibition of Eg5 by full length TPX2 slows Eg5 and inhibits microtubule sliding activity on antiparallel microtubule overlaps. Proper regulation of Eg5 and Kif15 by full length TPX2 thus leads to formation of a functional bipolar spindle. In the presence of TPX2 710 (Right panels), microtubules are nucleated in the vicinity of chromosomes. But, absence of TPX2 C-terminus fails to localize Eg5 and Kif15 on the spindle microtubules properly. In the presence of TPX2 710, reduced targeting of Kif15 prevents Kif15 dependent parallel bundle formation and prevents proper formation of stable K fiber. Tpx2-710 inhibits Eg5 molecules less effectively and the results in excessive Eg5 activity which causes disorganized and multi-polar spindles.

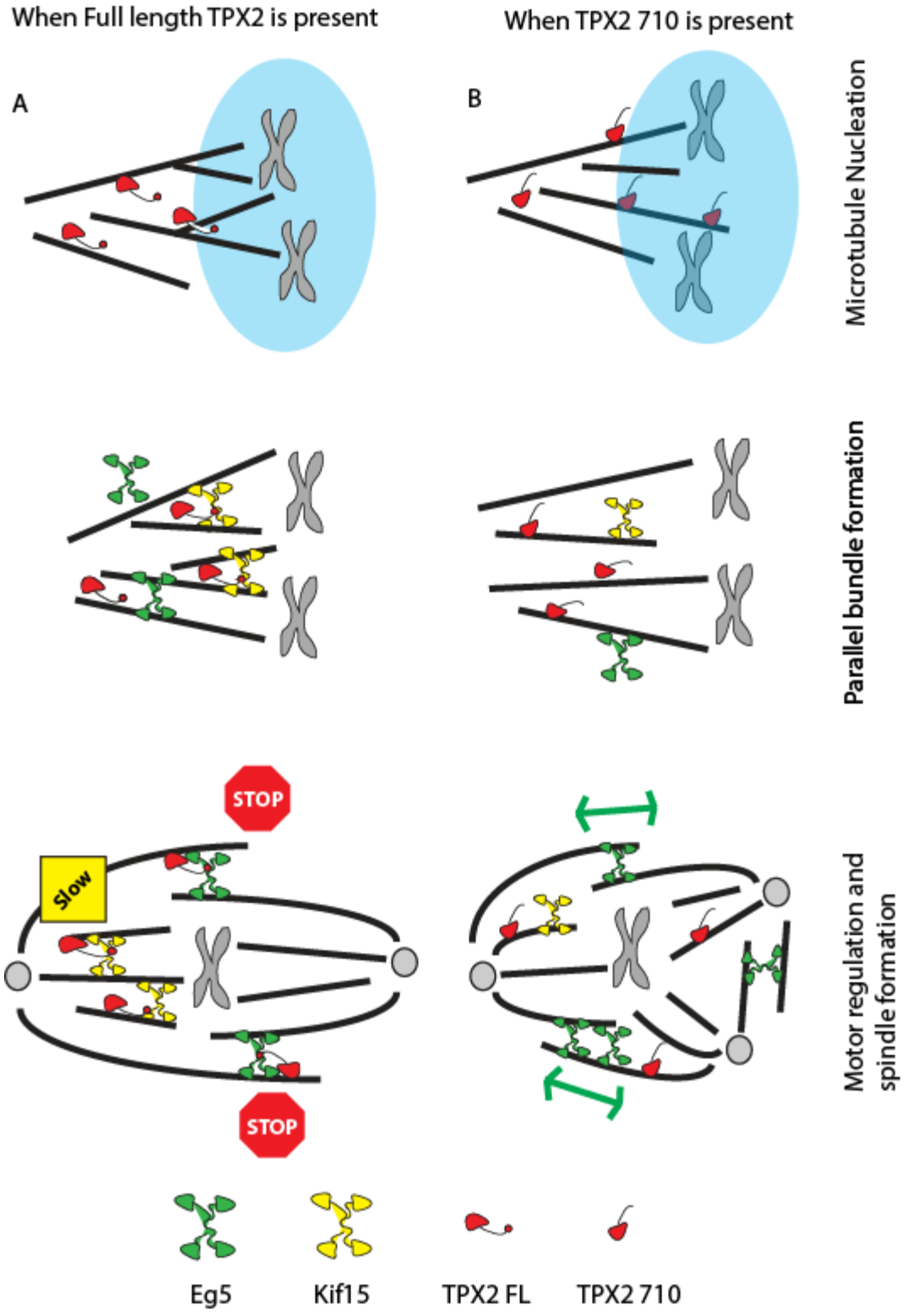
When Full length TPX2 is present
When TPX2 710 is present
A
B
Microtubule Nucleation
Parallel bundle formation
Motor regulation and spindle formation
STOP
Slow
STOP
Eg5
Kif15
TPX2 FL
TPX2 710

Figure 4.1 Proposed Model. Schematic representation of spindle formation in the presence of full length TPX2 (Left panels) and TPX2-710 (Right panels). Top row shows the microtubule nucleation around the chromosomes. Middle row shows the recruitment of motors Eg5 and Kif15 onto spindle microtubules and formation of microtubule bundles. Bottom row shows the regulation of motor activity by full length TPX2 and TPX2-710 and the resulting spindle morphology.

BIBLIOGRAPHY

Barlan, K., Rossow, M.J., and Gelfand, V.I. (2013). The journey of the organelle: teamwork and regulation in intracellular transport. Curr. Opin. Cell Biol. *25*, 483–488.

Bayliss, R., Sardon, T., Vernos, I., and Conti, E. (2003). Structural basis of Aurora-A activation by TPX2 at the mitotic spindle. Mol. Cell *12*, 851–862.

Bird, A.W., and Hyman, A.A. (2008). Building a spindle of the correct length in human cells requires the interaction between TPX2 and Aurora A. J. Cell Biol. *182*, 289–300.

Blangy, A., Lane, H.A., d'Hérin, P., Harper, M., Kress, M., and Nigg, E.A. (1995). Phosphorylation by p34cdc2 regulates spindle association of human Eg5, a kinesin-related motor essential for bipolar spindle formation in vivo. Cell *83*, 1159–1169.

Block, S.M., Goldstein, L.S., and Schnapp, B.J. (1990). Bead movement by single kinesin molecules studied with optical tweezers. Nature *348*, 348-352

Borisy, G.G. (1978). Polarity of microtubules of the mitotic spindle. J. Mol. Biol. *124*, 565–570.

Brouhard, G.J., Stear, J.H., Noetzel, T.L., Al-Bassam, J., Kinoshita, K., Harrison, S.C., Howard, J., and Hyman, A.A. (2008). XMAP215 is a processive microtubule polymerase. Cell *132*, 79–88.

Brunet, S., Sardon, T., Zimmerman, T., Wittmann, T., Pepperkok, R., Karsenti, E., and Vernos, I. (2004). Characterization of the TPX2 domains involved in microtubule nucleation and spindle assembly in Xenopus egg extracts. Mol. Biol. Cell *15*, 5318–5328.

Cai, D., Verhey, K.J., and Meyhöfer, E. (2007). Tracking Single Kinesin Molecules in the Cytoplasm of Mammalian Cells. Biophys J *92*, 4137–4144.

Case, R.B., Rice, S., Hart, C.L., Ly, B., and Vale, R.D. (2000). Role of the kinesin neck linker and catalytic core in microtubule-based motility. Curr. Biol. *10*, 157–160.

Day, R.N., and Davidson, M.W. (2009). The fluorescent protein palette: tools for cellular imaging. Chem Soc Rev *38*, 2887–2921.

DeBonis, S., Skoufias, D.A., Lebeau, L., Lopez, R., Robin, G., Margolis, R.L., Wade, R.H., and Kozielski, F. (2004). In vitro screening for inhibitors of the human mitotic kinesin Eg5 with antimitotic and antitumor activities. Mol. Cancer Ther. *3*, 1079–1090.

Drechsler, H., and McAinsh, A.D. (2016). Kinesin-12 motors cooperate to suppress microtubule catastrophes and drive the formation of parallel microtubule bundles. Proc. Natl. Acad. Sci. U.S.A. *113*, E1635-1644.

Drechsler, H., McHugh, T., Singleton, M.R., Carter, N.J., and McAinsh, A.D. (2014). The Kinesin-12 Kif15 is a processive track-switching tetramer. Elife *3*, e01724.

Eckerdt, F., Eyers, P.A., Lewellyn, A.L., Prigent, C., and Maller, J.L. (2008). Spindle pole regulation by a discrete Eg5-interacting domain in TPX2. Curr. Biol. *18*, 519–525.

Euteneuer, U., and McIntosh, J.R. (1981). Structural polarity of kinetochore microtubules in PtK1 cells. J. Cell Biol. *89*, 338–345.

Eyers, P.A., and Maller, J.L. (2004). Regulation of Xenopus Aurora A activation by TPX2. J. Biol. Chem. *279*, 9008–9015.

Ferenz, N.P., Paul, R., Fagerstrom, C., Mogilner, A., and Wadsworth, P. (2009). Dynein antagonizes eg5 by crosslinking and sliding antiparallel microtubules. Curr. Biol. *19*, 1833–1838.

Ferenz, N.P., Gable, A., and Wadsworth, P. (2010). Mitotic functions of kinesin-5. Semin. Cell Dev. Biol. *21*, 255–259.

Gable, A., Qiu, M., Titus, J., Balchand, S., Ferenz, N.P., Ma, N., Collins, E.S., Fagerstrom, C., Ross, J.L., Yang, G., et al. (2012). Dynamic reorganization of Eg5 in the mammalian spindle throughout mitosis requires dynein and TPX2. Mol. Biol. Cell *23*, 1254–1266.

Garrett, S., Auer, K., Compton, D.A., and Kapoor, T.M. (2002). hTPX2 is required for normal spindle morphology and centrosome integrity during vertebrate cell division. Curr. Biol. *12*, 2055–2059.

Gayek, A.S., and Ohi, R. (2016). CDK-1 Inhibition in G2 Stabilizes Kinetochore-Microtubules in the following Mitosis. PLoS ONE *11*, e0157491.

Gerson-Gurwitz, A., Thiede, C., Movshovich, N., Fridman, V., Podolskaya, M., Danieli, T., Lakämper, S., Klopfenstein, D.R., Schmidt, C.F., and Gheber, L. (2011). Directionality of individual kinesin-5 Cin8 motors is modulated by loop 8, ionic strength and microtubule geometry. EMBO J. *30*, 4942–4954.

Goodwin, S.S., and Vale, R.D. (2010). Patronin regulates the microtubule network by protecting microtubule minus ends. Cell *143*, 263–274.

Goshima, G. (2011). Identification of a TPX2-like microtubule-associated protein in Drosophila. PLoS ONE *6*, e28120.

Goshima, G., and Vale, R.D. (2003). The roles of microtubule-based motor proteins in mitosis: comprehensive RNAi analysis in the Drosophila S2 cell line. J. Cell Biol. *162*, 1003–1016.

Goshima, G., Nédélec, F., and Vale, R.D. (2005). Mechanisms for focusing mitotic spindle poles by minus end-directed motor proteins. J. Cell Biol. *171*, 229–240.

Goshima, G., Mayer, M., Zhang, N., Stuurman, N., and Vale, R.D. (2008). Augmin: a protein complex required for centrosome-independent microtubule generation within the spindle. J. Cell Biol. *181*, 421–429.

Groen, A.C., Needleman, D., Brangwynne, C., Gradinaru, C., Fowler, B., Mazitschek, R., and Mitchison, T.J. (2008). A novel small-molecule inhibitor reveals a possible role of kinesin-5 in anastral spindle-pole assembly. J. Cell. Sci. *121*, 2293–2300.

Gruss, O.J., and Vernos, I. (2004). The mechanism of spindle assembly: functions of Ran and its target TPX2. J. Cell Biol. *166*, 949–955.

Gruss, O.J., Carazo-Salas, R.E., Schatz, C.A., Guarguaglini, G., Kast, J., Wilm, M., Le Bot, N., Vernos, I., Karsenti, E., and Mattaj, I.W. (2001). Ran induces spindle assembly by reversing the inhibitory effect of importin alpha on TPX2 activity. Cell *104*, 83–93.

Gruss, O.J., Wittmann, M., Yokoyama, H., Pepperkok, R., Kufer, T., Silljé, H., Karsenti, E., Mattaj, I.W., and Vernos, I. (2002). Chromosome-induced microtubule assembly mediated by TPX2 is required for spindle formation in HeLa cells. Nat. Cell Biol. *4*, 871–879.

van Heesbeen, R.G.H.P., Raaijmakers, J.A., Tanenbaum, M.E., Halim, V.A., Lelieveld, D., Lieftink, C., Heck, A.J.R., Egan, D.A., and Medema, R.H. (2016). Aurora A, MCAK, and Kif18b promote Eg5-independent spindle formation. Chromosoma.

Heidemann, S.R., and McIntosh, J.R. (1980). Visualization of the structural polarity of microtubules. Nature *286*, 517–519.

Helenius, J., Brouhard, G., Kalaidzidis, Y., Diez, S., and Howard, J. (2006). The depolymerizing kinesin MCAK uses lattice diffusion to rapidly target microtubule ends. Nature *441*, 115–119.

Hinrichs, M.H., Jalal, A., Brenner, B., Mandelkow, E., Kumar, S., and Scholz, T. (2012). Tau protein diffuses along the microtubule lattice. J. Biol. Chem. *287*, 38559–38568.

Hirokawa, N., and Noda, Y. (2008). Intracellular transport and kinesin superfamily proteins, KIFs: structure, function, and dynamics. Physiol. Rev. *88*, 1089–1118.

Hirokawa, N., Noda, Y., Tanaka, Y., and Niwa, S. (2009). Kinesin superfamily motor proteins and intracellular transport. Nat. Rev. Mol. Cell Biol. *10*, 682–696.

Holmfeldt, P., Brattsand, G., and Gullberg, M. (2002). MAP4 counteracts microtubule catastrophe promotion but not tubulin-sequestering activity in intact cells. Curr. Biol. *12*, 1034–1039.

Honnappa, S., Gouveia, S.M., Weisbrich, A., Damberger, F.F., Bhavesh, N.S., Jawhari, H., Grigoriev, I., van Rijssel, F.J.A., Buey, R.M., Lawera, A., et al. (2009). An EB1-binding motif acts as a microtubule tip localization signal. Cell *138*, 366–376.

Hoyt, M.A., He, L., Loo, K.K., and Saunders, W.S. (1992). Two Saccharomyces cerevisiae kinesin-related gene products required for mitotic spindle assembly. J. Cell Biol. *118*, 109–120.

Hyman, A., Drechsel, D., Kellogg, D., Salser, S., Sawin, K., Steffen, P., Wordeman, L., and Mitchison, T. (1991). Preparation of modified tubulins. Meth. Enzymol. *196*, 478–485.

Illenberger, S., Drewes, G., Trinczek, B., Biernat, J., Meyer, H.E., Olmsted, J.B., Mandelkow, E.M., and Mandelkow, E. (1996). Phosphorylation of microtubule-associated proteins MAP2 and MAP4 by the protein kinase p110mark. Phosphorylation sites and regulation of microtubule dynamics. J. Biol. Chem. *271*, 10834–10843.

Kaláb, P., Pralle, A., Isacoff, E.Y., Heald, R., and Weis, K. (2006). Analysis of a RanGTP-regulated gradient in mitotic somatic cells. Nature *440*, 697–701.

Kapitein, L.C., Peterman, E.J.G., Kwok, B.H., Kim, J.H., Kapoor, T.M., and Schmidt, C.F. (2005). The bipolar mitotic kinesin Eg5 moves on both microtubules that it crosslinks. Nature *435*, 114–118.

Kapitein, L.C., Kwok, B.H., Weinger, J.S., Schmidt, C.F., Kapoor, T.M., and Peterman, E.J.G. (2008). Microtubule cross-linking triggers the directional motility of kinesin-5. J. Cell Biol. *182*, 421–428.

Kapoor, T.M., Mayer, T.U., Coughlin, M.L., and Mitchison, T.J. (2000). Probing spindle assembly mechanisms with monastrol, a small molecule inhibitor of the mitotic kinesin, Eg5. J. Cell Biol. *150*, 975–988.

Kashina, A.S., Scholey, J.M., Leszyk, J.D., and Saxton, W.M. (1996). An essential bipolar mitotic motor. Nature *384*, 225.

Komarova, Y., Lansbergen, G., Galjart, N., Grosveld, F., Borisy, G.G., and Akhmanova, A., (2005). EB1 and EB3 control CLIP dissociation from the ends of growing microtubules. Mol. Biol. Cell. *16*. 5334-5345.

Korneev, M.J., Lakämper, S., and Schmidt, C.F. (2007). Load-dependent release limits the processive stepping of the tetrameric Eg5 motor. Eur. Biophys. J. *36*, 675–681.

Kufer, T.A., Silljé, H.H.W., Körner, R., Gruss, O.J., Meraldi, P., and Nigg, E.A. (2002). Human TPX2 is required for targeting Aurora-A kinase to the spindle. J. Cell Biol. *158*, 617–623.

Kwok, B.H., Kapitein, L.C., Kim, J.H., Peterman, E.J.G., Schmidt, C.F., and Kapoor, T.M. (2006). Allosteric inhibition of kinesin-5 modulates its processive directional motility. Nat. Chem. Biol. *2*, 480–485.

Larson, A.G., Naber, N., Cooke, R., Pate, E., and Rice, S.E. (2010). The conserved L5 loop establishes the pre-powerstroke conformation of the Kinesin-5 motor, eg5. Biophys. J. *98*, 2619–2627.

Lawrence, C.J., Dawe, R.K., Christie, K.R., Cleveland, D.W., Dawson, S.C., Endow, S.A., Goldstein, L.S.B., Goodson, H.V., Hirokawa, N., Howard, J., et al. (2004). A standardized kinesin nomenclature. J. Cell Biol. *167*, 19–22.

Ledbetter, M.C., and Porter, K.R. (1963). A "MICROTUBULE" IN PLANT CELL FINE STRUCTURE. J. Cell Biol. *19*, 239–250.

Ledbetter, M.C., and Porter, K.R. (1964). Morphology of Microtubules of Plant Cell. Science *144*, 872–874.

Lowry, O.H., Rosebrough, N.J., Farr, A.L., and Randall, R.J. (1951). Protein measurement with the Folin phenol reagent. J. Biol. Chem. *193*, 265–275.

Ma, N., Tulu, U.S., Ferenz, N.P., Fagerstrom, C., Wilde, A., and Wadsworth, P. (2010). Poleward transport of TPX2 in the mammalian mitotic spindle requires dynein, Eg5, and microtubule flux. Mol. Biol. Cell *21*, 979–988.

Ma, N., Titus, J., Gable, A., Ross, J.L., and Wadsworth, P. (2011). TPX2 regulates the localization and activity of Eg5 in the mammalian mitotic spindle. J Cell Biol *195*, 87–98.

Maiato, H., Fairley, E.A.L., Rieder, C.L., Swedlow, J.R., Sunkel, C.E., and Earnshaw, W.C. (2003). Human CLASP1 is an outer kinetochore component that regulates spindle microtubule dynamics. Cell *113*, 891–904.

Makrides, V., Massie, M.R., Feinstein, S.C., and Lew, J. (2004). Evidence for two distinct binding sites for tau on microtubules. Proc. Natl. Acad. Sci. U.S.A. *101*, 6746–6751.

Markus, S.M., Kalutkiewicz, K.A., and Lee, W.-L. (2012). She1-mediated inhibition of dynein motility along astral microtubules promotes polarized spindle movements. Curr. Biol. *22*, 2221–2230.

Mayer, T.U., Kapoor, T.M., Haggarty, S.J., King, R.W., Schreiber, S.L., and Mitchison, T.J. (1999). Small molecule inhibitor of mitotic spindle bipolarity identified in a phenotype-based screen. Science *286*, 971–974.

Mitchison, T.J. (1993). Localization of an exchangeable GTP binding site at the plus end of microtubules. Science *261*, 1044–1047.

Mitchison, T., and Kirschner, M. (1984). Dynamic instability of microtubule growth. Nature *312*, 237–242.

Nogales, E., and Zhang, R. (2016). Visualizing microtubule structural transitions and interactions with associated proteins. Curr. Opin. Struc. Biol. *37*. 90-96

O'Connell, C.B., Loncarek, J., Kaláb, P., and Khodjakov, A. (2009). Relative contributions of chromatin and kinetochores to mitotic spindle assembly. J. Cell Biol. *187*, 43–51.

Paschal, B.M., Obar, R.A., and Vallee, R.B. (1989). Interaction of brain cytoplasmic dynein and MAP2 with a common sequence at the C terminus of tubulin. Nature *342*, 569–572.

Petry, S., Groen, A.C., Ishihara, K., Mitchison, T.J., and Vale, R.D. (2013). Branching microtubule nucleation in Xenopus egg extracts mediated by augmin and TPX2. Cell *152*, 768–777.

Piehl, M., Tulu, U.S., Wadsworth, P., and Cassimeris, L. (2004). Centrosome maturation: measurement of microtubule nucleation throughout the cell cycle by using GFP-tagged EB1. Proc. Natl. Acad. Sci. U.S.A. *101*, 1584–1588.

Raaijmakers, J.A., and Medema, R.H. (2014). Function and regulation of dynein in mitotic chromosome segregation. Chromosoma *123*, 407–422.

Reid, T.A., Schuster, B.M., Mann, B.J., Balchand, S.K., Plooster, M., McClellan, M., Coombes, C.E., Wadsworth, P., and Gardner, M.K. (2016). Suppression of microtubule assembly kinetics by the mitotic protein TPX2. J. Cell. Sci. *129*, 1319–1328.

Rice, S., Lin, A.W., Safer, D., Hart, C.L., Naber, N., Carragher, B.O., Cain, S.M., Pechatnikova, E., Wilson-Kubalek, E.M., Whittaker, M., et al. (1999). A structural change in the kinesin motor protein that drives motility. Nature *402*, 778–784.

Roof, D.M., Meluh, P.B., and Rose, M.D. (1992). Kinesin-related proteins required for assembly of the mitotic spindle. J. Cell Biol. *118*, 95–108.

Roostalu, J., Hentrich, C., Bieling, P., Telley, I.A., Schiebel, E., and Surrey, T. (2011). Directional switching of the kinesin Cin8 through motor coupling. Science *332*, 94–99.

Rusan, N.M., Fagerstrom, C.J., Yvon, A.M., and Wadsworth, P. (2001). Cell cycle-dependent changes in microtubule dynamics in living cells expressing green fluorescent protein-alpha tubulin. Mol. Biol. Cell. *12*. 971-980.

Roostalu, J., Cade, N.I., and Surrey, T. (2015). Complementary activities of TPX2 and chTOG constitute an efficient importin-regulated microtubule nucleation module. Nat. Cell Biol. *17*, 1422–1434.

Sawin, K.E., LeGuellec, K., Philippe, M., and Mitchison, T.J. (1992). Mitotic spindle organization by a plus-end-directed microtubule motor. Nature *359*, 540–543.

Schaar, B.T., Chan, G.K., Maddox, P., Salmon, E.D., and Yen, T.J. (1997). CENP-E function at kinetochores is essential for chromosome alignment. J. Cell Biol. *139*, 1373–1382.

Schatz, C.A., Santarella, R., Hoenger, A., Karsenti, E., Mattaj, I.W., Gruss, O.J., and Carazo-Salas, R.E. (2003). Importin alpha-regulated nucleation of microtubules by TPX2. EMBO J. *22*, 2060–2070.

Schmidt, J.C., Kiyomitsu, T., Hori, T., Backer, C.B., Fukagawa, T., and Cheeseman, I.M. (2010). Aurora B kinase controls the targeting of Astrin-SKAP complex to bioriented kinetochores. J. Cell. Biol. *191*. 269-280.

Scrofani, J., Sardon, T., Meunier, S., and Vernos, I. (2015). Microtubule nucleation in mitosis by a RanGTP-dependent protein complex. Curr. Biol. *25*, 131–140.

Sindelar, C.V., Budny, M.J., Rice, S., Naber, N., Fletterick, R., and Cooke, R. (2002). Two conformations in the human kinesin power stroke defined by X-ray crystallography and EPR spectroscopy. Nat. Struct. Biol. *9*, 844–848.

Skoufias, D.A., DeBonis, S., Saoudi, Y., Lebeau, L., Crevel, I., Cross, R., Wade, R.H., Hackney, D., and Kozielski, F. (2006). S-trityl-L-cysteine is a reversible, tight binding inhibitor of the human kinesin Eg5 that specifically blocks mitotic progression. J. Biol. Chem. *281*, 17559–17569.

Spittle, C., Charrasse, S., Larroque, C., and Cassimeris, L. (2000). The interaction of TOGp with microtubules and tubulin. J. Biol. Chem. *275*. 20748-20753

Stumpff, J., Wagenbach, M., Franck, A., Asbury, C.L., and Wordeman, L. (2012). Kif18A and chromokinesins confine centromere movements via microtubule growth suppression and spatial control of kinetochore tension. Dev. Cell *22*, 1017–1029.

Sturgill, E.G., and Ohi, R. (2013). Kinesin-12 differentially affects spindle assembly depending on its microtubule substrate. Curr. Biol. *23*, 1280–1290.

Sturgill, E.G., Das, D.K., Takizawa, Y., Shin, Y., Collier, S.E., Ohi, M.D., Hwang, W., Lang, M.J., and Ohi, R. (2014). Kinesin-12 Kif15 targets kinetochore fibers through an intrinsic two-step mechanism. Curr. Biol. *24*, 2307–2313.

Subramanian, R., Wilson-Kubalek, E.M., Arthur, C.P., Bick, M.J., Campbell, E.A., Darst, S.A., Milligan, R.A., and Kapoor, T.M. (2010). Insights into antiparallel microtubule crosslinking by PRC1, a conserved nonmotor microtubule binding protein. Cell *142*, 433–443.

Tanenbaum, M.E., Macůrek, L., Janssen, A., Geers, E.F., Alvarez-Fernández, M., and Medema, R.H. (2009). Kif15 cooperates with eg5 to promote bipolar spindle assembly. Curr. Biol. *19*, 1703–1711.

Trieselmann, N., Armstrong, S., Rauw, J., and Wilde, A. (2003). Ran modulates spindle assembly by regulating a subset of TPX2 and Kid activities including Aurora A activation. J. Cell. Sci. *116*, 4791–4798.

Tsai, M.-Y., Wiese, C., Cao, K., Martin, O., Donovan, P., Ruderman, J., Prigent, C., and Zheng, Y. (2003). A Ran signalling pathway mediated by the mitotic kinase Aurora A in spindle assembly. Nat. Cell Biol. *5*, 242–248.

Tulu, U.S., Fagerstrom, C., Ferenz, N.P., and Wadsworth, P. (2006). Molecular requirements for kinetochore-associated microtubule formation in mammalian cells. Curr. Biol. *16*, 536–541.

Uteng, M., Hentrich, C., Miura, K., Bieling, P., and Surrey, T. (2008). Poleward transport of Eg5 by dynein-dynactin in Xenopus laevis egg extract spindles. J. Cell Biol. *182*, 715–726.

Vale, R.D., Reese, T.S., and Sheetz, M.P. (1985). Identification of a novel force generating protein Kinesin, involved in microtubule based motility. *42*, 39-50.

Vanneste, D., Takagi, M., Imamoto, N., and Vernos, I. (2009). The role of Hklp2 in the stabilization and maintenance of spindle bipolarity. Curr. Biol. *19*, 1712–1717.

Waitzman, J.S., and Rice, S.E. (2014). Mechanism and regulation of kinesin-5, an essential motor for the mitotic spindle. Biol. Cell *106*, 1–12.

Walczak, C.E., and Heald, R. (2008). Mechanisms of mitotic spindle assembly and function. Int. Rev. Cytol. *265*, 111–158.

Wang, Z., and Sheetz, M.P. (2000). The C-terminus of tubulin increases cytoplasmic dynein and kinesin processivity. Biophys. J. *78*, 1955–1964.

Weinger, J.S., Qiu, M., Yang, G., and Kapoor, T.M. (2011). A nonmotor microtubule binding site in kinesin-5 is required for filament crosslinking and sliding. Curr. Biol. *21*, 154–160.

Welburn, J.P.I. (2013). The molecular basis for kinesin functional specificity during mitosis. Cytoskeleton (Hoboken) *70*, 476–493.

van den Wildenberg, S.M.J.L., Tao, L., Kapitein, L.C., Schmidt, C.F., Scholey, J.M., and Peterman, E.J.G. (2008). The homotetrameric kinesin-5 KLP61F preferentially crosslinks microtubules into antiparallel orientations. Curr. Biol. *18*, 1860–1864.

Wittmann, T., Boleti, H., Antony, C., Karsenti, E., and Vernos, I. (1998). Localization of the kinesin-like protein Xklp2 to spindle poles requires a leucine zipper, a microtubule-associated protein, and dynein. J. Cell Biol. *143*, 673–685.

Wittmann, T., Wilm, M., Karsenti, E., and Vernos, I. (2000). TPX2, A novel xenopus MAP involved in spindle pole organization. J. Cell Biol. *149*, 1405–1418.

Wood, K.W., Sakowicz, R., Goldstein, L.S., and Cleveland, D.W. (1997). CENP-E is a plus end-directed kinetochore motor required for metaphase chromosome alignment. Cell *91*, 357–366.

Wordeman, L., Wagenbach, M., and von Dassow, G. (2007). MCAK facilitates chromosome movement by promoting kinetochore microtubule turnover. J. Cell Biol. *179*, 869–879.

Yvon, A.M., Wadsworth, P., and Jordan, M.A. (1999). Taxol suppresses dynamics of individual microtubules in living human tumor cells. Mol. Biol. Cell *10*, 947–959.

Zanic, M., Widlund, P.O., Hyman, A.A., and Howard, J. (2013). Synergy between XMAP215 and EB1 increases microtubule growth rates to physiological levels. Nat. Cell Biol. *15*, 688–693.

Zhu, C., Zhao, J., Bibikova, M., Leverson, J.D., Bossy-Wetzel, E., Fan, J., Abraham, R.T., and Jiang, W. (2005). Functional analysis of human microtubule-based motor proteins, the kinesins and dyneins, in mitosis/cytokinesis using RNA interference. Mol. Biol. Cell. *16*, 3187-3199.